B-Physics Event Selection for the ATLAS High Level Trigger

John Baines[1], Andrea Baratella[2], Brigitte Epp[3], Simon George[4], Vasile Mihai Ghete[3], Leanne Guy[5], Saul Gonzalez[6], David Hutchcroft[4], Paolo Morettini[2], Armin Nairz[3], Fabrizio Parodi[2], Sijin Qian[6], Flora Rizatdinova[7], Diana Scannicchio[8], Matthias Sessler[9], Peter Sherwood[10], Sergey Sivoklokov[7], Maria Smizanska[11], Weidong Li[4]

Abstract

The ATLAS *B*-physics trigger relies on the partial reconstruction of *B* decays in order to select semi-exclusively specific channels of interest. The trigger is initiated by a muon from the LVL1 trigger which is confirmed at LVL2, firstly in the muon detector and then in association with an Inner Detector (ID) track. The next step is an un-guided search for tracks in the ID. In this note various candidate algorithms are assessed for implementation in the LVL2 trigger and Event Filter (EF). The track search can be initiated from the inside of the ID, using information from the Pixel detector or from the outside using information from the Transition Radiation Tracker (TRT). The result of the initial search is a set of tracks the parameters of which form seeds for extrapolation into the Semi-Conductor Tracker (SCT) and subsequently into the TRT, for tracks initiated at the inside, or into the Pixel detector for tracks initiated from the TRT. Three channels of interest for physics studies are used as examples of the trigger selection process: $B_d \to \pi^+\pi^-$ and *B* decays including the subsequent decays $D_s \to \phi^0(K^+K^-)\pi^-$ and $J/\psi \to e^+e^-$. The overall performance of the track reconstruction algorithms and LVL2 and EF selections are characterized in terms of efficiency for the signal channel, trigger rate and execution time.

1. Rutherford Appleton Laboratory, Chilton, Didcot, UK
2. Università di Genova e I.N.F.N., Genova, Italy.
3. Institut für Experimentalphysik der Leopold-Franzens-Universität Innsbruck, Austria.
4. Royal Holloway, University of London, Egham, UK.
5. CERN, Geneva, Switzerland.
6. University of Wisconsin, Madison, Wisconsin, USA.
7. Institute of Nuclear Physics, Moscow State University, Moscow, Russia.
8. Università di Pavia e I.N.F.N., Pavia, Italy.
9. Lehrstuhl für Informatik V, Universität Mannheim, Germany.
10. Department of Physics and Astronomy, University College London, UK.
11. Department of Physics, Lancaster University, Lancaster, UK.

1 Introduction

This note summarizes the status and overall performance of algorithms for the ATLAS *B*-physics Higher Level Trigger (**HLT**). The *B*-physics selection is initiated by a muon from the LVL1 trigger which is confirmed at LVL2, firstly in the muon detector and then in association with an Inner Detector (**ID**) track. This selection is summarized, more details can be found in Ref.[1]. The next step is an un-guided search for tracks in the ID. These tracks are used to reconstruct selected decay channels semi-exclusively. The parameters of tracks are combined in order to identify specific parent particles characterised by invariant mass. This note focuses on three channels whose selection relies on track reconstruction in the ID. Various candidate track reconstruction algorithms have been assessed for suitability for implementation in the LVL2 trigger and Event Filter, both fast algorithms specific to the trigger (some of which are suitable for implementation on FPGAs) and algorithms taken from offline reconstruction code. A brief description of these algorithms is given and their performance summarized based on measurements of efficiency for signal events which would pass an offline selection, trigger rate and execution time. In addition parameters relevant to data flow and architectural design issues are also provided. In previous work, efficiencies and rates were obtained using a modified version of the offline Inner Detector reconstruction program `XKalman` [5] and timing information was limited. In this note, results produced with algorithms developed specifically for the trigger are presented.

The following channels are considered:

- $B_d \rightarrow \pi^+\pi^-$
- $D_s \rightarrow \phi^0(K^+K^-)\pi^-$
- $J/\psi \rightarrow e^+e^-$

These channels can be triggered using only the inner detector track information in addition to the LVL1 muon. Channels which require additional information from the muon spectrometer or calorimeters are not covered by this note. The selection for these channels has been divided into two stages. The first stage is based on tracks reconstructed by the candidate LVL2 trigger algorithms. Results are also given for a second stage of selection, suitable for the EF, based on tracks reconstructed by the offline reconstruction program xKalman. The main aim of this note is to demonstrate a viable *B*-physics trigger for these three channels by showing that the candidate algorithms give reasonably high efficiency for signal events, a sufficiently low trigger rate (approaching that of previous work), and an execution time compatible with their intended use. These are the three key parameters in the optimization of the algorithms and trigger cuts.

Rates quoted in this note are calculated by measuring the fraction of events that pass the trigger cuts from a sample of $B \rightarrow \mu X$ events with pile-up at low luminosity (10^{33} $cm^{-2}s^{-1}$). This is then normalised to 9 kHz, the nominal output rate from the LVL2 RoI-guided muon trigger. This calculation is based on a number of assumptions which will be discussed in more detail in Section 4

The ATLAS inner detector [2] consists of a **pixel** detector nearest the interaction point, a Semi-Conductor Tracker (**SCT**) at intermediate radius and a Transition Radiation Tracker (**TRT**) composed of straw detectors on the outside. The Pixel detector and micro-strip detectors of the SCT are both constructed from Silicon wafers and are collectively know as the **Si**-detector. The TRT provides electron identification based on sensitivity to transition radiation. Fast algorithms have been developed to perform un-guided searches for tracks in the TRT and Pixel detectors and for extrapolating these tracks into the Si detector.

There are some interesting issues for the HLT architecture arising from the *B*-physics trigger. It has been shown that the baseline *B*-physics trigger makes requirements on bandwidth for data movement and CPU power that are likely to dominate the LVL2 trigger resources at low luminosity [ref.]. The optimum boundary between LVL2 and the Event Filter is not yet clear. For the purposes of this note we assume that latency is one of the key differences between LVL2 and EF: LVL2 algorithms must execute in times of the order of 10 ms, while Event Filter algorithms can take longer at around 1 s. Another possible difference is technology. While both LVL2 and EF currently anticipate that commodity computers will be sufficiently performant for on-line processing, the LVL2 trigger also has the option to supplement the processing power with FPGAs. The availability of tracking data for an un-guided track search depends on the bandwidth available to transfer data from the LVL2 ROBs to a LVL2 processor. We have algorithms to initiate track searches in the pixel detector and alternatively in the TRT. Both of these are then followed by extrapolation into the other parts of the inner detector. It may be advantageous to run both algorithms simultaneously if parallel processing is possible and sufficient network bandwidth is available.

2 Overview of the *B*-physics trigger strategy

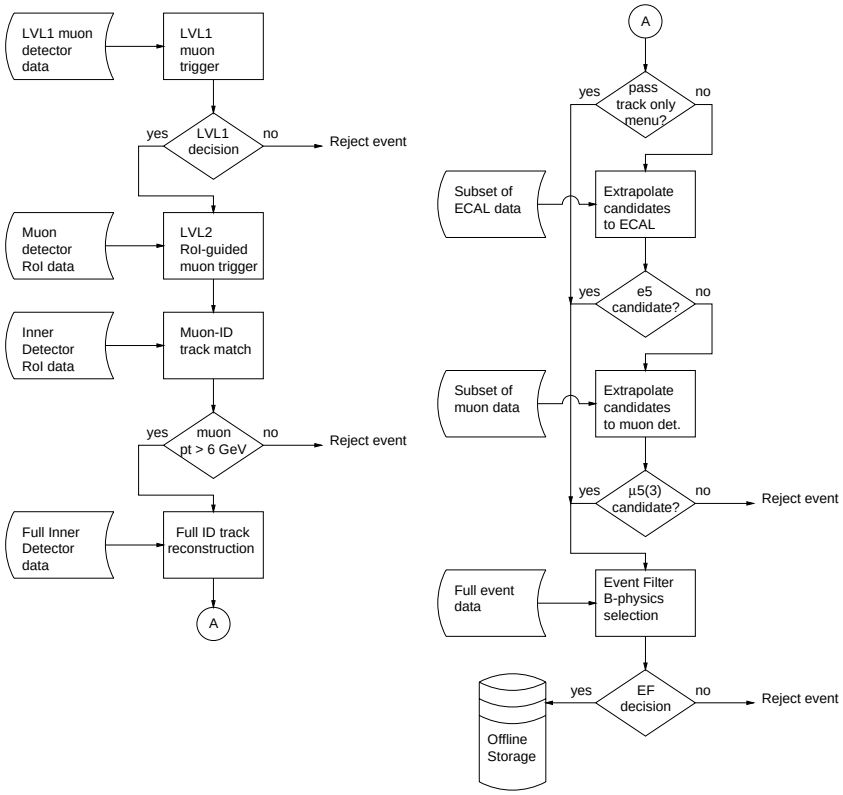

Figure 1: Logical overview of the *B*-physics trigger

The low-luminosity *B*-physics trigger menu will only be used in the following case:

- the LVL1 trigger includes a MU6;
- the LVL2 trigger confirms a μ6 trigger.

The precision muon detector and the inner detector are used to confirm the muon RoI at LVL2. If this succeeds, an un-guided track search will be performed in the inner detector. Without the constraints of RoI guidance, tracks can be found down to very low p_T (e.g. 0.5 GeV). These tracks are the objects required by the *B*-physics trigger menu in addition to μ6, as shown in Table 1. It is assumed that the LVL2 muon RoI confirmation will reduce the muon rate from the 23 kHz provided by LVL1 to 9 kHz. The rates in the table depend on this assumption and include the effect of pile-up at low luminosity.

The rates after the LVL2 selection are given in Table 1. They are all taken from Chapter 10 of [6]. There is little overlap between the trigger items so the total rate is approximately equal to the sum of the rates for the individual triggers.

Table 1: The entire Physics TDR table for reference.

	Trigger requirements	**Selected *B*-decay channels**	**Rate (Hz)**
Hadron channels	$D_s \to \phi(K^+K^-)\pi$, 3 hadrons $p_T > 1.5$ GeV, loose mass cuts	$B_s \to D_s\,\pi$, $B_s \to D_s\,a_1$	190
	2 hadrons $p_T > 4$ GeV, loose mass, angle and $\sum p_T$ cuts	$B_d \to \pi\pi$	80
Electron channels	*ee* pair, $p_T > 0.5$ GeV, identification by TRT, 2.0 GeV < m(*ee*) < 3.8 GeV	$b\bar{b} \to \mu B_d(J/\psi(ee)K^0)$	310
	single *e*, $p_T > 5$ GeV, identification in TRT+ECAL of electron reconstructed with $p_T > 4$ GeV in the Inner Detector	$b\bar{b} \to e$ $B_d(J/\psi(\mu\mu)K^0)$	93 [51 from true electrons, 42 from wrongly-identified hadrons]
Muon channels	second μ ($p_T > 5$ GeV, $\|\eta\| < 2.5$) identification in muon chambers + matching with the Inner Detector	$B_d \to J/\psi(\mu\mu)(K/K^*)$, $B_s \to J/\psi(\mu\mu)\phi$, $B \to \mu\,\mu$, $B \to K^{0*}\mu\mu$, *etc.*, $\Lambda_b \to \Lambda^0\,J/\psi(\mu\mu)$, $B_c \to J/\psi(\mu\mu)\,\pi$	170 [80 from *b/c*, 90 from K/π]
Total LVL2 *B*-physics trigger rate			840 Hz

3 Data-sets

The results presented in this note were produced using produced using data simulated using a full GEANT based simulation of the inner detector using the DICE code (version dice98_2). The physics simulations was performed by the ATGENB package (atgenb_98_1) based on PYTHIA.

The version of the ID design used for the simulation is that described in the section 3 of Ref. [2][1]. The data samples used are as follows, the cross sections for the processes are given in Table 2:

- $B_d \rightarrow \pi^+\pi^-$
- $B \rightarrow D_s\pi$
- $B_d \rightarrow J/\psi(e^+e^-)K_S$
- $bb \rightarrow \mu X$

More details of the data-set productions can be found in Ref. [4]. The acceptance of the ID extends to $|\eta| < 2.5$, and so the signal samples were restricted to this eta range. The events were required to have:

- b and $\bar{b}$ produced within $|\eta|<2.5$ and with $p_T > 6$ GeV
- a muon from b or $\bar{b}$ with $p_T > 6$ GeV
- all products of the signal B-meson decay lie within $|\eta|<2.5$
- all π, K and e daughters of the B-meson decay to have $p_T > 0.5$GeV.

Table 2: cross-sections for the different processes.

Process	Cross-Section (μb)	Rate at 10^{33} cm^{-2}s^{-1} (Hz)
$B_d \rightarrow \pi^+\pi^-$	8.4×10^{-6}	8.4×10^{-3}
$B \rightarrow D_s\pi$	1.281×10^{-5}	1.281×10^{-2}
$B_d \rightarrow J/\psi(e^+e^-)K_S$	3.8×10^{-6}	3.8×10^{-3}
$bb \rightarrow \mu X$	1.9	1900

1. There have since been some changes to the details of the design of the ID which are listed in section 8.3.1 of [3]. The detector simulation used for this study includes the effects of inefficiency and noise in the SCT and pixel layers. The effects of miss-alignment have not been included in the present study.

4 LVL2 muon trigger

The *B*-physics trigger begins at LVL2 with confirmation of any LVL1 muon RoIs. This can be performed in several stages, firstly using only muon data, and then by combining muon and ID information. The main background comes from muons with p_T below the LVL1 threshold of 6 GeV which are nevertheless accepted due to the finite p_T resolution at LVL1. At LVL2 most of these muons with p_T below threshold can be rejected thanks to the improved p_T resolution. The remaining background is mainly muons from decays in flight of pions and kaons. Some rejection of this background is possible by detecting a miss-match between the track measured in the muon system and the ID track.

4.1 Calculation of trigger rates

The rates quoted in this note are calculated by measuring the fraction of events that pass a trigger selection from a background sample of $bb \rightarrow \mu X$ events with pile-up at low luminosity (10^{33} $cm^{-2}s^{-1}$). This fraction is then converted to a rate based on an assumption of the rate of events passing the $p_T > 6$ GeV threshold of the LVL2 muon trigger.

In previous calculations of B trigger rates, [2][3][6], a LVL2 muon trigger rate of 9 kHz was estimated assuming a cut on the p_T of the reconstructed ID track, but without using muon-ID matching cuts. The main contributions to this rate are shown in Table 3. For consistency, the same normalisation is used for the calculation of the rates presented in this note.

Table 3: The main contributions to the LVL2 muon rate quoted in Ref. [3].

	Rate (kHz)		
Source	**Barrel**	**End-cap**	**Total**
$K/\pi \rightarrow \mu$	**2.4**	**3.2**	**5.6**
$b \rightarrow \mu$	**1.0**	**1.3**	**2.3**
$c \rightarrow \mu$	**0.5**	**0.6**	**1.1**
Total	**3.9**	**5.1**	**9.0**

The rates derived in this ways are somewhat pessimistic for two reasons:

- The contribution from K/π decays in flight can be reduced by applying cuts based on the matching of the parameters of the muon and ID track segments.
- The fractions of events selected by the B trigger selections have been measured for a sample of $B \rightarrow \mu X$ events which represent only the $b \rightarrow \mu$ component of the events passing the LVL2 muon trigger. The tracking trigger rate is dominated by combinatorial background, so it is sensitive to the p_T spectrum and charged particle multiplicity. The main background process $K/\pi \rightarrow \mu$ have a softer charged particle p_T spectrum than $b \rightarrow \mu$ so the trigger rate is likely to be lower than an extrapolation from $bb \rightarrow \mu X$ alone would suggest.

Recent studies[1] using muon algorithms suitable for the LVL2 trigger in the barrel region ($|\eta| < 1$) have shown that good rejection can be achieved against muons from K and π decays in flight whilst maintaining good efficiency for prompt muons. The efficiency of the muon reconstruction algorithm μFAST is shown in Figure 2 (top) as a function of muon p_T for prompt

muons and muons from π and K decay. Also shown, Figure 2 (bottom), is the efficiency for reconstructing and associating a Si track. These studies give a LVL2 muon trigger rate of 2.1kHz in the barrel region cf. the rate of 3.9 kHz given in Table 3. Studies using trigger algorithms have e yet to be extended to the forward muon detector. However, measurements using simple trigger-like algorithms within the offline framework suggest that an overall LVL2 muon trigger rate of 5 kHz should be attainable, giving a 45% reduction in the trigger rates quoted in this note.

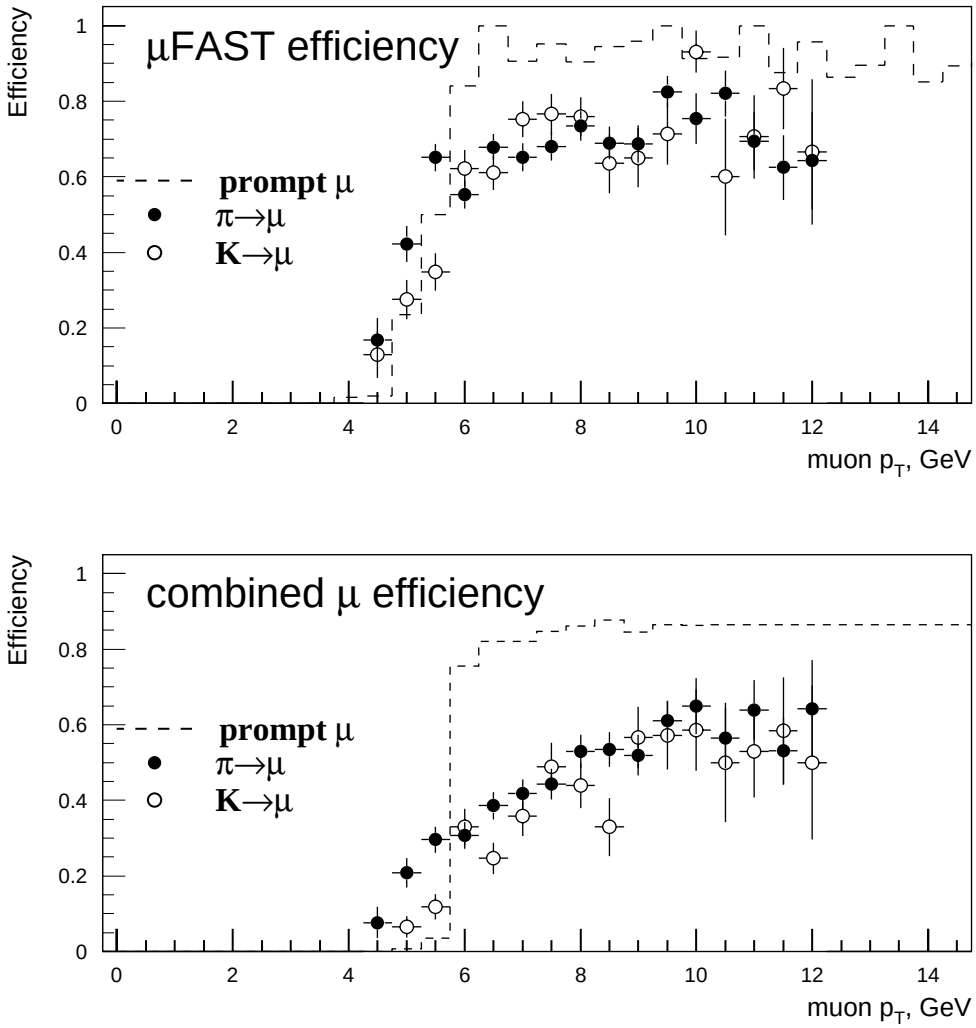

Figure 2: The efficiency as a function of p_T for a muon passing the LVL1 selection to be reconstruction by the LVL2 muon algorithm μFAST (top) and for subsequently associating a Si track (bottom). The efficiency is shown for prompt muons and muons from π and K decays.

4.2 Muon guidance to the B trigger

In addition to initiating the *B*-physics trigger, the muon information is utilized in the *B*-trigger for the following:

- To define the Z co-ordinate of the interaction point that produced the $b\bar{b}$ pair. This is used by the pixel-scan to reduce the number of hit combinations to be considered.

- For some channels (e.g. $B_d \rightarrow \pi^+\pi^-$), cuts on track positions relative to the trigger muon are made to discriminate against cases where the track and muon are in a jet.

The LVL2 RoI-guided muon trigger algorithm was not available when the tracking trigger studies in the following sections were carried out. Instead, the result of the muon trigger was simulated in two ways.

- For the pixel scan, the MC truth parameters of the muon were used instead. This will not influence the results significantly because the Z vertex position resolution (see [1]) of the LVL2 muon trigger is expected to be much better than the width of the Z-vertex constraint, which is typically 1 cm.
- For the cuts on the track position relative to the trigger muon, the resolution of the reconstructed track parameters is important. The level-2 muon was simulated by creating a fake RoI of width $\Delta\phi$=0.1 rad around the true muon direction and searching for a Si track in this region. In the case of more than one Si track, the one closest to the muon is used, using the definition for proximity of $\Delta R = \sqrt{\Delta\phi^2 + \Delta\eta^2}$. The reconstructed parameters of this track were used in the event selection cuts. This track-finding requirement results in a muon trigger efficiency of 99.1±0.3% for $B_d \rightarrow \pi^+\pi^-$ signal events and 99.3±0.2% for $bb \rightarrow \mu X$ background events. It is emphasised that this requirement and efficiency do not relate very closely to the real LVL2 muon trigger. The resolutions of the track parameters are worse than will be the case for the level-2 muon, where there will be additional information from the muon detector.

5 LVL2 track search

The track search can be initiated from the outside of the ID using TRT information or from the inside using Pixel data. A **full-scan** is performed to search the entire volume of the TRT or pixel detector respectively. The result of the full-scan is a set of tracks the parameters of which form **seeds** for extrapolation into the SCT. For TRT seeds the extrapolation continues into the pixels. For Pixel seeds, the TRT scan is run independently and matching[1] between Si and TRT track segments is then performed.

The requirements of Inner Detector track reconstruction algorithms for *B* physics differ from those for track searches guided by a LVL1 or LVL2 Region of Interest (**RoI**) in that the entire detector volume must be searched and the minimum p_T for track reconstruction is, in general, much lower in the *B*-physics trigger. The requirement to reconstruct invariant mass demands good efficiency and track reconstruction quality. Various candidate algorithms have been assessed for suitability for implementation in the LVL2 trigger and Event Filter, both fast algorithms specific to the trigger (some of which are suitable for implementation on FPGAs) and algorithms taken from offline reconstruction code. The assessment of performance is based on measurements of efficiency for signal events which would pass an offline selection, trigger rate and execution time. A summary of the selections and their performance are given here.

This section describes the track search which is common to all *B*-physics channels. Several Feature EXtraction (**FEX**) algorithms have been developed and tested. A brief description of each algorithm is given below, followed by a summary of their performance in terms of efficiency, speed and track multiplicity. The trigger algorithms and their performance are described more fully elsewhere.

5.1 Algorithms

TRT full scan

A histogram is formed by counting hits (active straws) along candidate track trajectories. Tracks are identified as peaks in the histogram. A fit is performed to the selected points to produce track parameters. This method is implemented in the initial stage of XKalman, and as a fast look-up table method which has been developed for possible implementation on FPGA co-processors. For more details on the look-up table method, see [8]. XKalman is documented in [9].

Pixel full scan

This algorithm uses only information from the pixel detector. The input data are the pixel cluster positions produced by a separate data preparation step [14]. In the first step of the full-scan algorithm, clusters are combined in pairs. All combinations are tested of one cluster per layer in the inner two planes of the barrel and in two of the end-cap planes. A pair is retained if the trajectory extrapolation inwards passes within a given distance of the interaction point. A track is

1. This matching is not proposed as an optimal tracking solution, but it is the only method available at the time of writing.

formed if a hit is found close to the extrapolated track into the third layer barrel layer or in one of the outer pixel end-cap layers. In both cases the extrapolation is linear. The interaction point is well defined in the transverse plane by the beam geometry. But the interaction region has a large spread along the beam direction (σ_Z = 6.1 cm). Guidance from the LVL2 muon trigger can be used to determine the position in Z of the interaction point and so limit the track search to those tracks which extrapolate back to within a small window in Z. This eliminates tracks which are not from either the primary interaction point or the *B*-decay vertex. For the results presented here, rather than using the reconstructed muon track, the true trajectory of the muon has been used. In this note, results are presented for three cases:

- no muon guidance;
- a window around the Z intercept of the muon trajectory of ΔZ = 0.4 cm;
- a window around the Z intercept of the muon trajectory of ΔZ = 1.0 cm;

More details of the pixel-scan algorithm can be found in [11].

Si Kalman Filter

This FEX is based on a Kalman filter algorithm [10]. A track search may be initiated by either an external or internal seed. For the purposes of the *B*-physics trigger, the Si-Kalman FEX uses either pixel or TRT tracks as external seeds in **pixel-seeded** or **TRT-seeded** mode respectively. The track segment is extended by adding nearby hits layer by layer. The algorithm can take into account multiple scattering, bremsstrahlung energy loss and inhomogenous magnetic field. More details can be found in [10].

Si Hough Transform

This algorithm is based on a FEX used for the electron trigger guided by a calorimeter RoI. The FEX was been modified to use TRT tracks as seeds and to extend the track search down to low p_T. This algorithm has been used for an initial evaluation of the $D_s \rightarrow \phi(K^+K^-)\pi$ trigger reported in Ref. [12]. Subsequent studies based on the Si-Kalman FEX have given much better performance, and it is these results that are included in this note.

Si Tree

A separate study can be found in [13]. The results of this algorithm for the $B_d \rightarrow \pi^+\pi^-$ channel show a slight improvement over the Si Kalman Filter in terms of rate and efficiency, with about half the execution time

Si to TRT Association

In the case of a pixel seed, it would be beneficial to continue the extrapolation of the track from the Si into the TRT in order to improve the track parameter resolution and benefit from the electron identification capability of the TRT. Electron identification is crucial for the $J/\psi \rightarrow e^+e^-$ trigger in order to reduce the combinatorial background from hadron tracks. Such an extension of the track would be possible using a modification of the Si Kalman filter FEX, or using the tree algorithm. However, currently no trigger code exists to perform this extrapolation. Instead, for the results presented in this note, an independent TRT full-scan has been performed and the Si and TRT track segments associated in a separate step. The association algorithm proceeds by ex-

trapolating each Si track to the radius (TRT barrel) or Z (TRT end-cap) of the inner-most hit on the TRT track segment and calculating the $\Delta\phi$ between the extrapolated track and the TRT straw position. The Si track with the smallest value of $|\Delta\phi| < 0.02$ Rad is chosen and associated to the TRT track.

5.2 Performance

The performance of the track reconstruction algorithms has been characterised in terms of the efficiency to find charged muons, pions and electrons in typical *B*-physics events and the execution time of the algorithm. Also important is the quality of the reconstructed track parameters, this has been evaluated from the width of the invariant mass peak for $B_d \rightarrow \pi^+\pi^-$ events.

5.2.1 Muon reconstruction

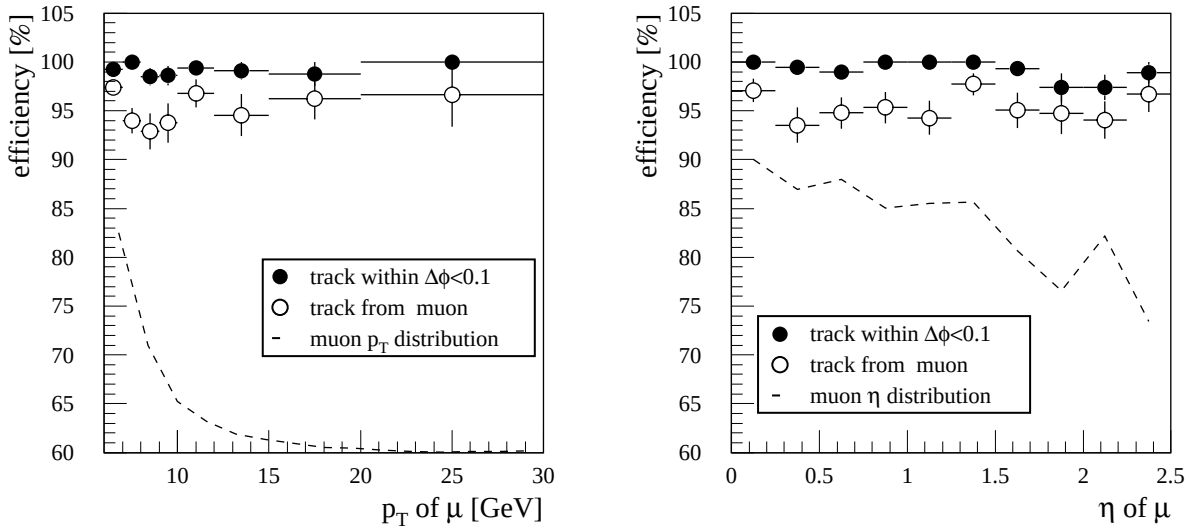

Figure 3: Efficiency to reconstruct a a muon in the ID within $\Delta\phi < 0.1$ of the true muon trajectory using the pixel-scan followed by Si-kalman shown as a function of p_T (left) and $|\eta|$ (right). The corresponding p_T and $|\eta|$ distributions of muons are also shown.The general trend in the $|\eta|$ distribution is slowly falling from left to right; the detailed structure reflects the low statistics available.

The efficiency to reconstruct a muon in the ID within $\Delta\phi < 0.1$ of the true muon trajectory is shown in Figure 3. In the case that more than one Si track is found in the ϕ–window, then the one closest to the muon is taken, using the definition for proximity of $\Delta R = \sqrt{\Delta\phi^2 + \Delta\eta^2}$ .The results were obtained using the pixel-scan followed by Si-kalman on $B_d \rightarrow \pi^+\pi^-$ events. The efficiency is show as a function of p_T (left) and $|\eta|$ (right). The mean efficiency to find a track inside this fake RoI is 99.1±0.3%, and 95.0±0.8% have the majority of hits contributed by the muon. The results for background events ($bb \rightarrow \mu X$) are consistent.

5.2.2 Pion reconstruction

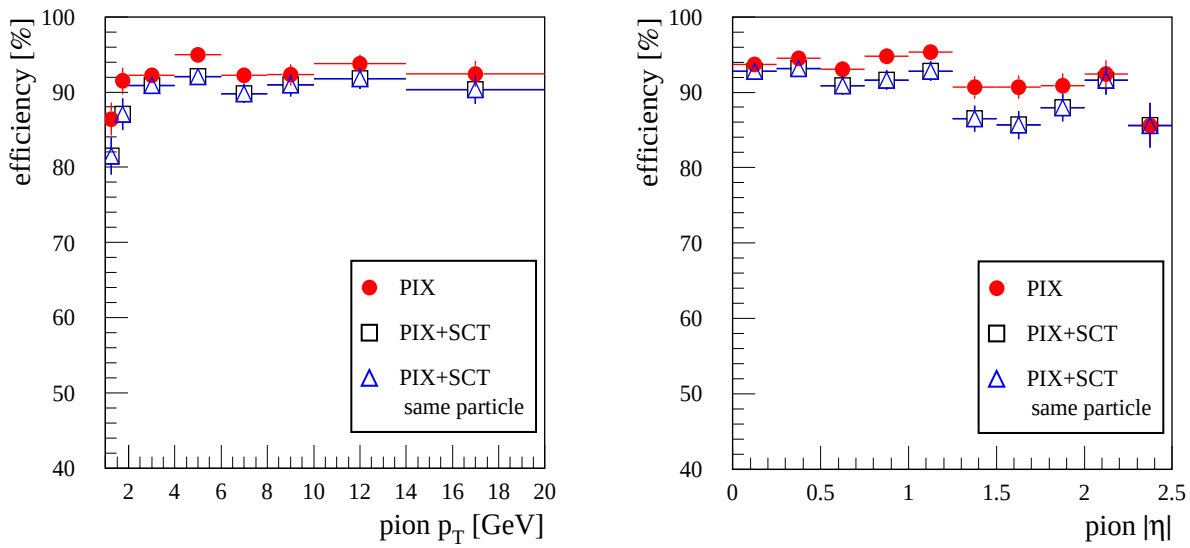

Figure 4: Track reconstruction efficiency by the Pixel scan and Si-Kalman algorithms, for charged pions from $B_d \rightarrow \pi^+\pi^-$ decays with $p_T > 0.5$ GeV versus generated p_T (left) and |η| (right).

The efficiency for the pixel-scan to reconstruct pions with $p_T > 1$ GeV from the decay $B_d \rightarrow \pi^+\pi^-$ is shown in Figure 4 as a function of the pion p_T (left) and | η | (right) for events with pile-up at low luminosity. Also shown is the efficiency for the pion to be reconstructed in the SCT by the Kalman FEX seeded by the pixel-scan. The average track reconstruction efficiency is 93% for the pixel-scan. On average 97% of these tracks are additionally reconstructed in the SCT, giving an average overall efficiency of 90%. These plots have been constructed by associating each track segment in the Pixels and SCT to the particle which contributed the majority of hits. The track segment is said to be due to this particle. A pion track is defined to be found if there is a reconstructed track associated to it. In some cases, when there is a high density of tracks, it is possible that track segments in the SCT and Pixel detectors are due to different particles. This causes errors in the parameters of the combined track-fit. Also shown in Figure 4 is the efficiency when both track segments are required to be due to the same particle. It can be seen that in almost all cases the Pixel and SCT track segments are from the same track.

Figure 5 shows corresponding plots of efficiency to find charged pions from $B_d \rightarrow \pi^+\pi^-$ versus p_T (left) and |η| (right) for track searches initiated by the TRT–LUT FEX (top) and the TRT-XK FEX (bottom). The average efficiency for both the TRT-LUT and TRT-XK scan to reconstruct pion tracks is 88% which is slightly lower than the corresponding value for the pixel scan. Of the tracks reconstructed by the TRT-LUT (TRT-XK) scan, on average 94.5% (97.5%) are additionally reconstructed in the Si detector (respectively), but an average of 5% of these tracks are due to a different particle from that reconstructed in the TRT. This gives an overall average efficiency for the TRT-LUT (TRT-XK) FEX and Si FEX to reconstruct the pion track of 79% (82%) respectively, which is ~10% lower than for a Pixel seeded reconstruction. However the loss of efficiency is predominantly in a small region of |η| corresponding to the transition from barrel to end-cap TRT geometry. There are a reduced number of TRT measurements along the track trajectory in this region. In addition the hits are divided between the TRT barrel and end-cap. Separate track segments are reconstructed in the TRT barrel and end-cap. At present no attempt is made to merge barrel and end-cap track segments. The threshold on the number of TRT hits required to form a track has been reduced in this transition region, which has the effect of main-

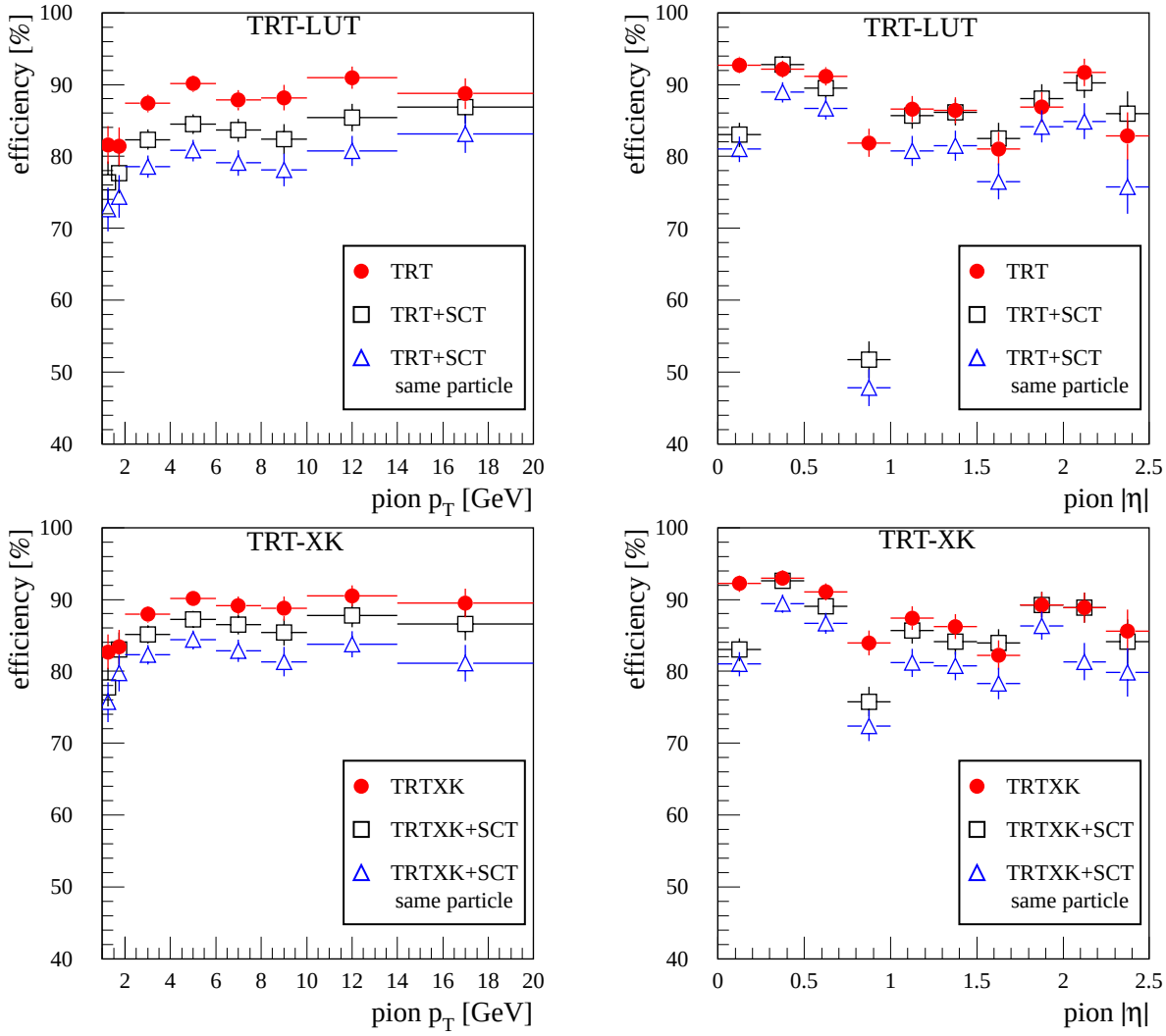

Figure 5: Track reconstruction efficiency by the TRT scan and Si-Kalman algorithms for charged pions from $B_d \to \pi^+\pi^-$ decays with p_T > 1 GeV versus generated p_T (left) and |η| (right). Results are shown for the TRT-LUT FEX (top) and the TRT-XK FEX (bottom).

taining the TRT efficiency. However the track quality is considerable reduced with the result that these tracks do not seed the Si FEX very effectively, and so the efficiency for the same track to be reconstructed in the Si is considerably reduced in this region

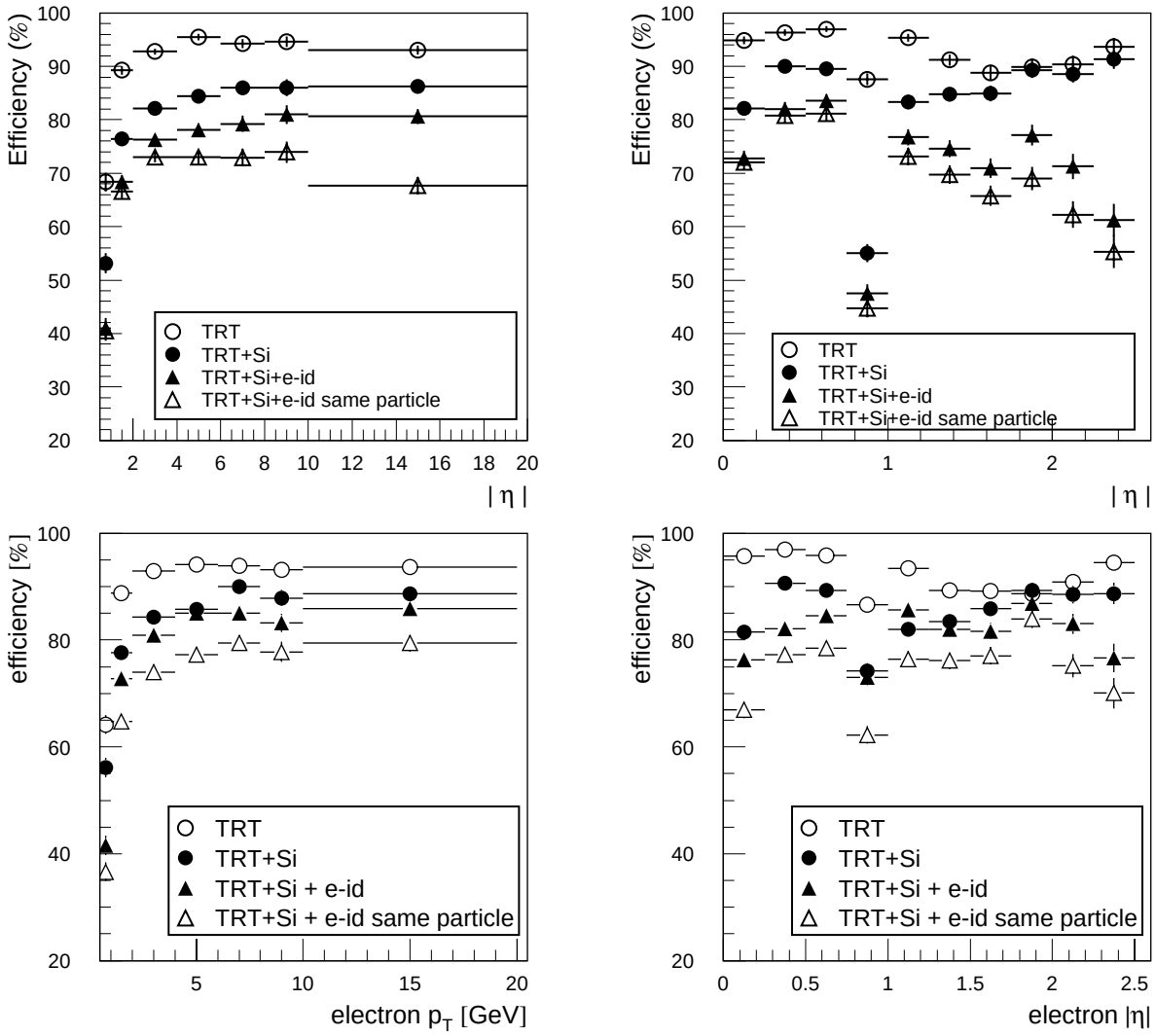

Figure 6: Efficiency for TRT-XK (top) and TRT-LUT (bottom) seeded track reconstruction versus p_T (left) and efficiency versus |η| (right) for electrons from J/ψ → e^+e^-. The plots are shown for electrons with p_T>0.5 (1GeV) for the right (left) plots respectively.

5.2.3 Electron reconstruction

The efficiency for reconstructing e^+ and e^- from $B_d \to J/\psi(e^+e^-)K_S$ decays is shown in Figure 6 as a function of p_T (left) and $|\eta|$ (right) for the TRT-scan plus Si-Kalman FEX. Results are shown for TRT-scans using the TRT-XK FEX (top) and TRT-LUT FEX (bottom) in events with pile-up at low luminosity. The average efficiency for the TRT-LUT (TRT-XK) FEX to reconstruct an electron with p_T > 1 GeV from $B_d \to J/\psi(e^+e^-)K_S$ decays is 92.9% (92.1%) (respectively). The parameters of the TRT FEX have been set so as to be reasonably efficient for electrons with a p_T of 1 GeV. However due

Table 4: TRT electron identification cuts based on the ratio of the number of hits passing the higher Transition Radiation threshold, N_{TR}, to the total number of hits on the track, N_{hits},

	N_{TR}/N_{hits} >	
Region	**TRT–LUT**	**TRT-XK**
$\|\eta\| < 0.8$	0.10	0.10
$0.8 < \|\eta\| < 1.4$	0.14	0.14
$1.4 < \|\eta\| < 2.0$	0.18	0.18
$2.0 < \|\eta\|$	0.18	0.20

to the effects of Bremsstrahlung energy loss, the efficiency increases with p_T until a p_T of ~5 GeV. The average efficiency for the track to be reconstructed by the Si FEX is 82.6% (85.4%) when seeded by the TRT-LUT (TRT-XK) FEX (respectively). Also shown in Figure 6 is the efficiency for tracks reconstructed by the Si to be correctly identified as electrons on the basis of the fraction of TR hits on the TRT track segment. The electron identification requirements are given in Table 4. The average efficiency to reconstruct an electron track and correctly identify it as an electron is 72.5% (81.2%) for the TRT-LUT (TRT-XK) FEX respectively. For 95.0% (90.5%) of these the tracks, the track segment reconstructed by the TRT-LUT (TRT-XK) FEX is due to the same particle as the reconstructed Si track, giving an overall efficiency for electron reconstruction of 68.9% (73.5%).

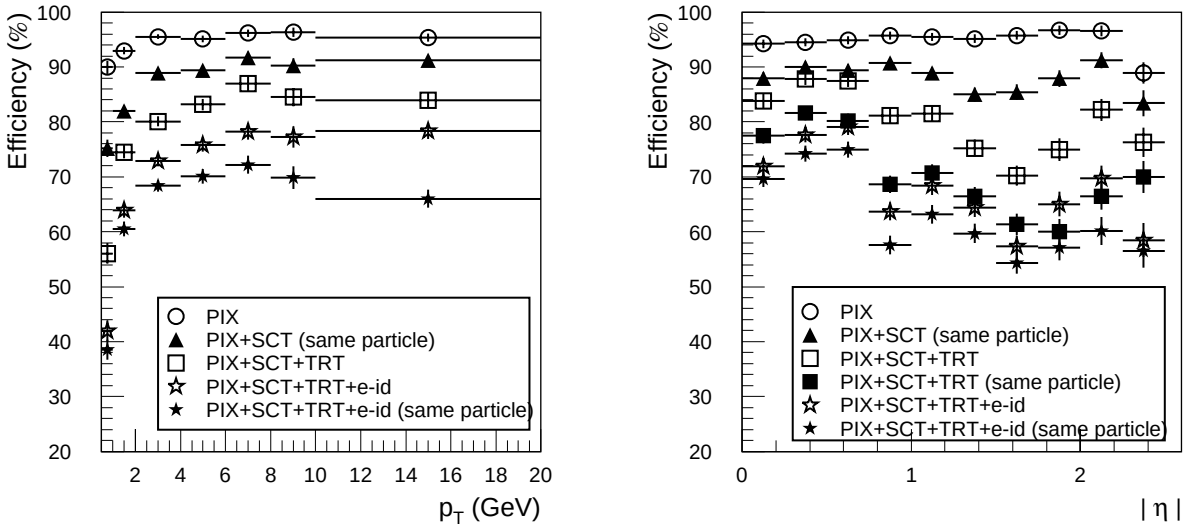

Figure 7: Efficiency as a function of p_T (left) and efficiency versus |η|(right) for e^+ and e^- from *B*->J/ψ decays in events with pile-up for the TRT-LUT plus Si-Kalman FEX.

The corresponding plots of efficiency for reconstructing e^+ and e^- from $B \rightarrow J/\psi$ decays using the pixel-scan plus Si-Kalman FEX are shown in Figure 7 as a function of p_T (left) and $|\eta|$ (right) in events with pile-up at low luminosity. The average efficiency for the pixel-scan to reconstruct an electron from $B_d \rightarrow J/\psi(e^+e^-)K_S$ is 95.0%. The average efficiency for the electron to be reconstructed by the SCT FEX seeded by the pixel-scan is 88.4%. Of these tracks, the same particle is reconstructed by the SCT and pixel detector in 99.9% of cases. Also shown in Figure 7 is the efficiency for an electron track to be reconstructed in the Si and for a TRT track to be associated. Of the electron tracks reconstructed in the Si, on average 91.7% are associated to a TRT track. The correct association of TRT and Si tracks is affected by Bremsstrahlung energy loss which can cause kinks in the track at the SCT/TRT boundary. Also the track fit to the TRT hits is constrained to the origin, which can cause a miss-measurement of the track trajectory in the cases where there has been a significant deviation of the particle from its initial trajectory. As a consequence, the associated Si and TRT tracks are due to the same particle in only 88.5% of cases. The associated track is correctly identified as an electron in 89.7% of cases, giving an overall efficiency for electron reconstruction of 64.3%.

5.2.4 Hit sharing

An important consideration in reducing the number of track candidates is whether reconstructed tracks are allowed to share hits. The TRT-XK and pixel-scan algorithms have been designed to resolve hit sharing during reconstruction. As part of the studies for this note, a post-processing step to merge track candidates sharing hits has also been added to the TRT-LUT algorithm.

In the case of the pixel scan, hit-sharing is resolved by choosing the hit combination that gives the smallest residual between the track extrapolated from the inner two layers and the hit in the third layer. The mean number of pixel seeds is shown inTable 5 for the cases when hit sharing is and is not allowed. Also shown are the efficiencies for reconstructing particles in $B \rightarrow D_s \rightarrow \phi^0(K^+K^-)\pi^-$ events with pile-up. It can be seen that allowing hit-sharing gives a significant increase in efficiency for reconstructing the D_s, due primarily to an increase in efficiency for reconstruction the K daughters of the ϕ. However there is a corresponding doubling of the number of track candidates when hit sharing is allowed, which has implications for the trigger rate. This will be discussed in Section 6.4.

Table 5: The mean number of pixel seeds in $B \rightarrow \mu X$ events with pile-up for the cases when hit sharing is and is not allowed and the corresponding efficiency for reconstructing tracks in $D_s \rightarrow \phi^0(K^+K^-)\pi^-$ events with pile-up.

Efficiency		No muon Guidance		With Muon Guidance (Δz<0.4cm)	
		No hit sharing	With hit Sharing	No hit sharing	With hit Sharing
Mean No. Tracks		38	90	18	36
Efficiency (%)	π from Ds	85.2	86.7	84.6	85.2
	K from Ds	80.4	87.4	81.4	86.4
	ϕ	74.4	85.6	75.3	83.8
	D_s	60.1	73.1	62.4	72.0

For the TRT-LUT FEX, two options have been implemented to resolve hit sharing. In order to save execution time, this post-processing step can be limited to only consider electron candidate tracks. In the case that two tracks share more than a given fraction of hits, either:

- the shortest track is rejected
- the tracks are merged and a new track-fit performed to the hits from the combined tracks..

Table 6: The effect of track merging on the mean number of tracks produced by the TRT-LUT FEX and on the efficiency for reconstructing both electrons from $J/\psi \rightarrow e^+e^-$ events with electron $p_T^{true} > 0.5$ GeV.

Track merging scheme	TRT-LUT		
	Mean number of e candidate tracks	Efficiency (%)	
		TRT–guided	pixel–guided
No track merging	57	87.3	75.7
Reject shorter track sharing >20% hits	50	85.2	75.2
Merge tracks sharing >20%hits	52	83.1	73.0

The results of this track merging step are shown in Table 6. There is a reduction in the number of electron track candidates by 12% if, when track candidates share more than 20% of hits, the shorter of two candidates is rejected. If, instead, the hits on the two track candidates are combined, and the track re-fit before track cuts re-applied, the number of track candidates is reduced by 9% with respect to the case with no track merging. As a result of the merging step there is a loss of efficiency for reconstructing both the e^+ and e^- tracks from $B_d \rightarrow J/\psi(e^+e^-)K_S$ of 2% and 4% for the two merging schemes respectively. For the results presented in this note, no track merging has been performed.

5.2.5 Track quality

An important consideration that is not revealed in the efficiency plots is the quality of track reconstruction. Figure 8 shows the $\pi^+\pi^-$ invariant mass distributions obtained for reconstructed pions with $p_T > 4.0$ GeV from $B_d \rightarrow \pi^+\pi^-$ decays for pixel-seeded reconstruction and using seeds from the TRT-LUT FEX. The results of Gaussian fits to the data are shown superimposed. The width of the mass peak is about a factor two bigger using TRT-guided track reconstruction than for pixel seeds. This is a consequence of multiple scattering and energy loss before the TRT due to interactions with the material of the inner detector. It is also a consequence of the fact that the TRT produces no η measurement in the barrel and has relatively poor η resolution in the end-caps, whereas the pixel detector yields relatively accurate seed information in all three dimensions. It may be possible to improve the track quality by modifying the use of TRT information for seeding the Si FEX. At present, only the information from three TRT hits is used to seed the Si track search and in the combined track fit to the Si and TRT points. By including all hits on the TRT track segment, it may be possible to improve the quality of the reconstructed tracks.

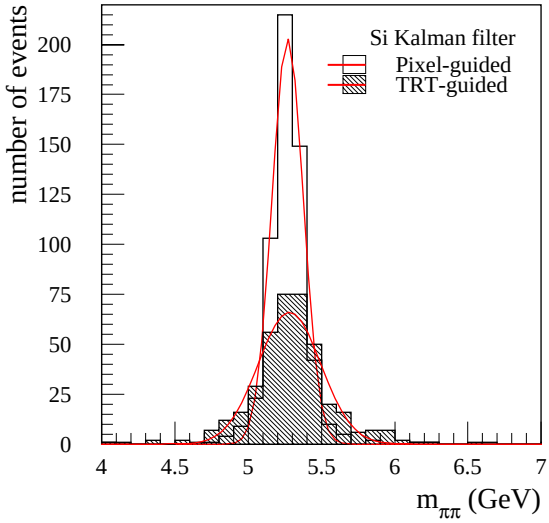

Figure 8: Reconstructed $\pi^+\pi^-$ invariant mass for track s from $B_d \rightarrow \pi^+\pi^-$ decays with $p_T(\pi) > 4$ GeV. The plot shows that the TRT-guided tracking gives worse mass resolution (213 ± 13 MeV) than the Pixel-guided tracking (106 ± 4 MeV)

5.3 Execution time

The execution times for the various algorithms have been measured on the following platforms:

- single CPU Pentium-III 450 MHz
    - 512K L2 cache
    - TMC TI6NBFV+ mother board
    - 128M 100MHz Memory
- single CPU Athlon 600MHz

Table 7: Mean execution times for TRT-seeded track searches. Times are shown for the TRT-scan, Si FEX, and the sum of these measured on a 600 MHz AMD Athlon and a 450 MHz PIII. Results are shown for TRT-LUT FEX and for the TRT-XK FEX and for various values of the p_T cut applied to TRT seeds. Also shown are the times when only electron candidates are used as seeds to the Si fex. The mean numbers of tracks reconstructed by the TRT-scan are also given.

		TRT–LUT FEX				TRT–XK FEX			
		all seeds			e-seeds	all seeds			e-seed
	p_T cut	0.5	1	1.5	0.5	0.5	1	1.5	0.5
	No. Seeds	171	82	54	57	114	56	38	32
Athlon (ms)	TRT-scan	150	150	150	150	399	344	326	399
	Si-Kalman	167	84	55	57	112	55	37	31
	Total	317	234	205	207	511	399	363	430
PIII (ms)	TRT-scan	236	236	236	236	580			580
	Si-kalman	265	129	86		171	81	54	
	Total	501	365	322		751			

Table 8: Mean execution times for pixel-seeded track searches. Times are shown for the pixel-scan, Si FEX, TRT-scan and for the association of Si and TRT track segments measured on a 600 MHz AMD Athlon and a 450 MHz PIII. Results are shown for pixel scans with and without muon guidance and for various values of the p_T cut applied to pixel seeds. Also shown is the mean number of tracks reconstructed by the pixel-scan.

		Without muon guidance			With muon guidance ($\Delta z < 1$ cm)		
	p_T cut (GeV)	0.5	1.0	1.5	0.5	1.0	1.5
	No. Seeds	78	29	16	39	16	10
Execution time (ms) Athlon	Pix-scan	166	38	25	22	12	11
	Si-Kalman	32	14	8	19	9	6
	Si total	198	52	33	41	21	17
	TRT-scan	150	150	150	150	150	150
	Si-TRT Assoc.	134	57	34	57	27	18
	Total	482	259	217	248	198	185
Execution time (ms) PIII	Pix-scan	297	52	18	50	19	18
	Si-kalman	89	32	14	47	19	14
	Si total	386	84	32	97	38	32
	TRT-scan	230	230	230	230	230	230
	Si-TRT Assoc.	214	76	28	107	42	28
	Total	830	390	290	434	310	290

- 512K L2 cache

- Microstart 6167 mother-board
- 128MB 100MHz memory

The code was compiled[1] with maximum optimization[2]. The timing measurements were made a

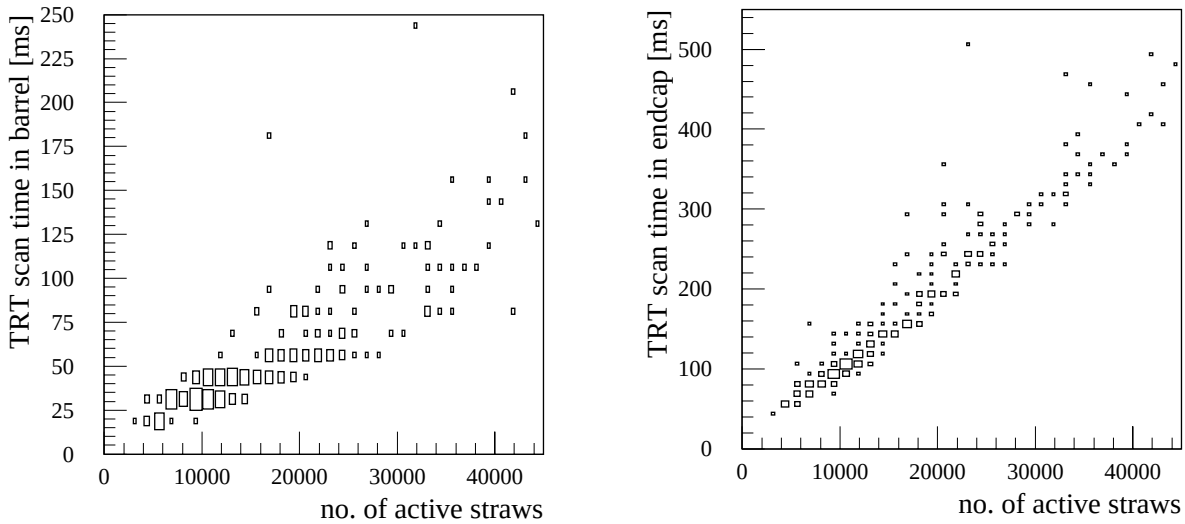

Figure 9: The execution time of the TRT-LUT full-scan in the TRT barrel (left) and TRT end-caps (right) as a function of the number of TRT hits. The measurements were made on a 450 MHz PIII using a sample of *B*–>μX events with pile-up at low luminosity.

using a sample of $B \rightarrow \mu X$ events with pile-up at low luminosity. The mean execution times are given in Table 7. The execution time for the TRT-LUT FEX scales linearly with the number of hits, as shown in Figure 9 (left). The TRT-XK FEX algorithm includes a hit-ordering step, and as a consequence the execution time scales a NlogN, see Figure 9 (right). The mean execution time on the PIII (Athlon) is 580 ms (400 ms) for the TRT-XK algorithm and 230 ms (150 ms) for the TRT-LUT FEX. The most CPU-intensive parts of the TRT-LUT FEX have also been implemented on FPGAs used both as a co-processor to a Pentium CPU and in the FPGA systems ENABLE++ and ATLANTIS [8]. These implementations offer a reduction in execution time by at least a factor 10.

1. The compiler used was using gcc / g++ version egcs-2.91.66 from egcs release 1.1.2.
2. The compiler optimization flags used with the Athlon were: *-s -static -O3 -fomit-frame-pointer -mpentiumpro -march=pentiumpro -malign-functions=4 -funroll-loops -fexpensive-optimizations -malign-double -fschedule-insns2 -mwide-multiply* and with the PIII: *-fnonnull-objects -O6 -fomit-frame-pointer -march=pentium -mcpu=pentium -malign-loops=2 -malign-jumps=2 -malign-functions=2*

The pixel-scan uses a combinatorial method and so the execution time contains contributions that scale as the second and third powers of occupancy as shown in Figure 11. It is therefore important to limit the number of point-combinations to be considered. The information from the LVL2 muon track can be used to determine the z position of the interaction point and so reduce the number of hit combinations to be tried and hence the execution time. The mean execution times with and without muon guidance are given in Table 8. Without muon guidance, the mean execution time of the pixel-scan on the PIII (Athlon) 300 ms (170 ms). With muon guidance ($\Delta z < 1$ cm) the execution time is 50 ms (23 ms) on the PIII (Athlon, respectively).

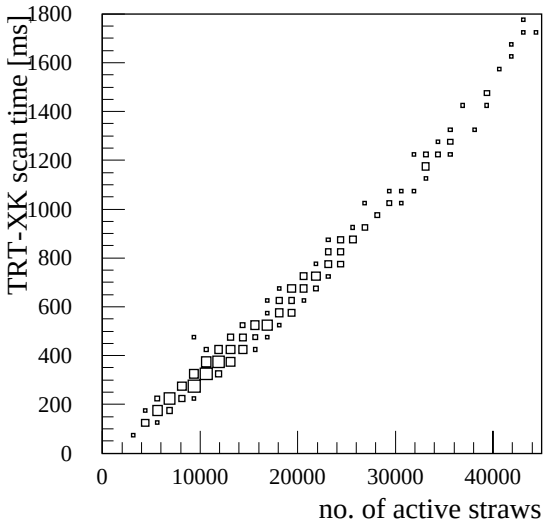

Figure 10: The execution time of the TRT-XK full-scan as a function of the number of TRT hits. The measurements were made on a 450 MHz PIII using a sample of $B \rightarrow \mu X$ events with pile-up at low

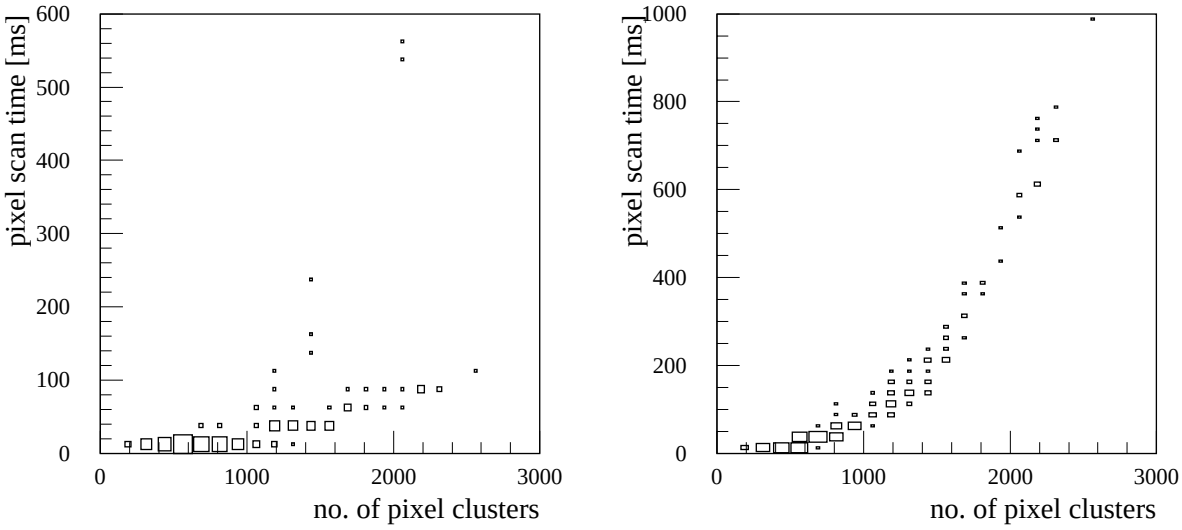

Figure 11: The execution time for the pixel-scan as a function of the number of clusters with (left) and without (right) muon guidance ($\Delta Z < 1$cm).The measurements were made on a 450 MHz PIII.

The Si-FEX takes a mean of ~0.8 ms (~0.5 ms) per pixel seed on the PIII (Athlon). A longer time of ~1.5 ms (~1 ms) per seed is required per TRT-seed on the PIII (Athlon), since in this case the track search encompasses the Pixels as well as the SCT. Distributions of the execution time per TRT seed and pixel seed are shown in Figure 12. A cut on the p_T of the Pixel or TRT track can be used to reduce the number of seeds and hence the overall execution time. The mean number of TRT seeds and Pixel seeds are given in Tables 8 and 7 respectively for a range of p_T-cut values together with the corresponding mean execution time for the Si-FEX. Results are shown in Table 8 for the pixel-scan with and without muon guidance. As a general rule, both the use of muon guidance and raising the pixel-p_T threshold will make the pixel algorithm faster and reduce the number of seeds passed on to the Si-Kalman FEX. At the lowest pixel-p_T threshold of 0.5 GeV, the number of seeds without muon guidance is about double what it is with muon

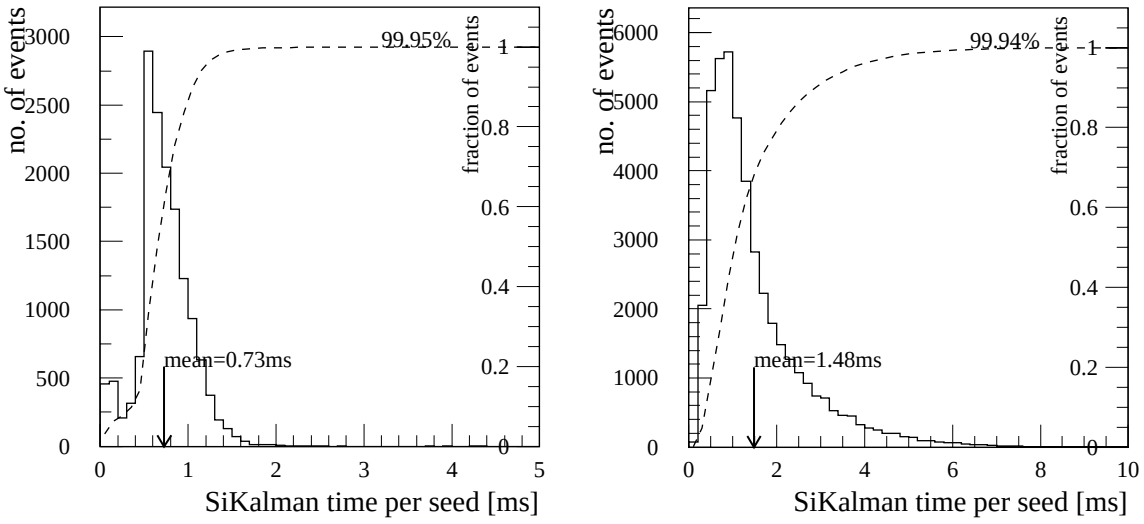

Figure 12: The distribution of the execution time of the Si-kalman FEX per pixel seed (left) and per TRT seed (right) measured on a 450 MHz PIII. Super-imposed are curves showing the fraction of seeds for which the execution time is below the given value. The number in the top right of the figure is the total fraction up to the right edge of the histogram.

guidance. However, if the pixel-p_T threshold is raised to 1.5 GeV the number of seeds is reduced to the same number irrespective of muon guidance. For the triggers involving only electron tracks, the number of TRT seeds can be reduced by using only TRT tracks passing electron identification cuts as seeds. The results shown in Table 7 for the TRT-XK FEX and TRT-LUT FEX. For the TRT-LUT FEX the number of seeds is ~50% higher.

Note that the above timing measurements do not include operations that may be considered to be pre-processing or data preparation, i.e. data collection and the formation of clusters and space points from strip / pixel addresses. These algorithms have been bench marked elsewhere; see for example [14]

Do we add timings for XKalman since it is used for EF results? Perhaps a few comments on the order of magnitude at least?

5.4 Conclusions on track search

The TRT scan has the advantage of an execution time that increases linearly with occupancy, whereas the pixel scan although faster on average, has contributions to the execution time that scale as the second and third power of the occupancy. The pixel scan does not suffer from a localised drop of efficiency or increase in fake tracks as the TRT does across its barrel-end-cap transition region. The pixel scan is intrinsically less robust as it requires hits in all three pixel planes to find a track, so it is sensitive to the pixel efficiency cubed. Plans are under way to investigate making this more robust by requiring a hit in the third pixel layer or the first SCT layer. The TRT has no such problem but instead suffers from material effects which seriously compromise its ability to make accurate measurements of track parameters with simple trigger algorithms. It also lacks the true 3D capabilities of the Pixel detector.

Algorithm times look promising; the times of the Pixel-scan using the muon RoI and the Si-Kalman seeded by this are compatible with times used in the Pilot Project modelling [ref]. It should also be noted that the TRT scan time can be significantly reduced by partial implementation on an FPGA co-processor. There are plans to investigate the implementation of some of the other tracking algorithms on FPGAs.

6 Trigger selections and performance

In this section trigger selections are given for three channels: $B_d \to \pi^+\pi^-$, $D_s \to \phi^0(K^+K^-)\pi^-$ and $J/\psi \to e^+e^-$. The performance of these selections is characterised in terms of the efficiency for a signal sample, the efficiency for events that would be selected offline, and the rate and execution time for a sample of $B \to \mu X$ events. All event samples include pile-up corresponding to running at low luminosity. Following the LVL2 track reconstruction described in the previous section, the selection process has been divided into the following three steps:

- LVL2 track selection
- LVL2 event selection
- Event Filter selection

The LVL2 selection uses tracks reconstructed by the algorithms described in Section 5, whilst the event filter selection is based on a track reconstruction by a modified version of the offline reconstruction programme `xKalman`.

In this section, firstly the data samples used for the efficiency and rate measurements are defined, then the common elements of the LVL2 track selection are outlined. The selections for the different channels are described in detail both at LVL2 and at the EF. A summary of efficiencies, rates and execution times is given at the end of this section.

6.1 Data samples

Table 9: The data samples used for the efficiency and rate measurements.

	Signal samples			
	$B_d \to \pi^+\pi^-$	$D_s \to \phi^0(K^+K^-)\pi^-$	$J/\psi \to e^+e^-$	$B \to \mu X$
Tapes	Y01319 files 1 to 8	Y24574 files 37,38,53,54 first 500 events per file	Y00350 files 1 to 16	Y00347
Events on tape	755	1989	4000	1607
Events with reconstructed μ			–	–
p_T cut	4 GeV	1.5 GeV	0.5 GeV	0.5
No. events in signal sample (events passing p_T cut)	714	786	4000	1607
No. events in offline sample (events passing offline selection)		166	536	-

The samples referred to in this section are defined as follows:

Signal sample

Events from the appropriate signal data-sets after the requirement for a reconstructed track in the fake muon RoI and after the application of cuts to the true p_T of the *B*-decay products matching the values of the p_T cuts used in the offline analysis. The value of the p_T cut is given in Table 9. Further details are given in the appropriate section below.

Offline sample

More important than the “absolute” efficiency for signal events, is the efficiency for the subset of signal events, as defined above, which would pass an offline selection. Such a selection will evolve with time. For the results presented here the offline selections presented in the Physics and Detector performance TDR [6] have been used. The selection cuts are listed in Appendix A. The efficiency of the trigger selection should be as high as possible for this subset of signal events to confirm that the trigger cuts are correlated with the offline cuts and no serious biases are introduced.

A subset of the signal sample, defined above, which additionally pass the offline selections used for the results presented in the Physics and Detector performance TDR [6]. Details of the selections are given in Appendix A.

Background

A sample of fully simulated $B \rightarrow \mu X$ events with pile-up [15].

All samples contain pile-up of minimum bias events corresponding to low luminosity running (10^{33} $cm^{-2}s^{-1}$).

6.2 Track selection

The first step, after track reconstruction at LVL2, is the application of track selection cuts. The serving tracks are input to a further stage of selection where parameters from two or more tracks are combined. This track selection step is important both to reduce the combinatorial background and to minimize the overall execution time. The following cut is common to all channels:

- $\mathbf{N_{Si}}$**:** The number of Si hits. For pixel seeded searches, at least 5 Si hits are required (2 SCT hits in addition to the three pixel hits required by the pixel-scan). For TRT seeded searches at least 3 Si hits are required.

Cuts may be also be applied to some or all of the following, depending on the channel, see Table 10:

- $\boldsymbol{p_T}$**:** The reconstructed p_T is required to be greater 0.5 GeV for the $\mathbf{J/\psi \rightarrow e^+e^-}$ trigger, greater than 1.5 GeV for the $D_s \rightarrow \phi^0(K^+K^-)\pi^-$ trigger and greater than 3.9 GeV for the $B_d \rightarrow \pi^+\pi^-$ trigger. These cuts remove low-p_T tracks and reduce the number of fake tracks formed by combinations of hits from more than one particle.
- The tracks reconstructed by the Si Kalman algorithm are required to have at least 2 SCT space points in addition to the three Pixel space points identified by the pixel scan

Table 10: The LVL2 track selection cuts for the different selections.

	$B_d \to \pi^+\pi^-$	$D_s \to \phi^0(K^+K^-)\pi^-$	$J/\psi \to e^+e^-$
p_T > (GeV)	3.9	1.5	0.5
d_0 < (cm)	–	1	–
z_0 < (cm)	–	20	–
ΔR > (cm)	0.2	0.2	–
R_1	-	-	see Table 4

- **d_0:** the closest approach of the reconstructed track to the origin. For the $D_s \to \phi^0(K^+K^-)\pi^-$ trigger, the reconstructed d_0 is required to be less than 1 cm.
- **z_0:** the z intercept of the track. For the $D_s \to \phi^0(K^+K^-)\pi^-$ trigger, the reconstructed z_0 is required to be less than 20 cm. [Simon: is this actually z on the helix at r=d0 according to our definition?]
- Δ**R**: the separation in ϕ–η space between the trigger muon and the Si Kalman track. For the $B_d \to \pi^+\pi^-$ and $D_s \to \phi^0(K^+K^-)\pi^-$ triggers, a cut is applied to require events to have a $\Delta R > 0.2$, where ΔR is defined by:
  $\Delta R = \sqrt{\Delta\phi^2 + \Delta\eta^2}$.
- **R_1**: The fraction of transition radiation hits on the TRT track segment, $R_1 = N_{TR} / N_{hits}$, where N_{TR} is the number of TR hits and N_{hits} the total number of hit son the TRT track segment. The cuts used to select electron candidate tracks for the $J/\psi \to e^+e^-$ trigger are given in Table 4.

6.3 $B_d \to \pi^+\pi^-$

The offline analyses currently planned for this channel put the following requirements on the trigger:

- Good efficiency for $B_d \to \pi^+\pi^-$ decays in which the daughters have $p_T > 4.0$ GeV. For this reason a p_T cut of 3.9 GeV has been applied to the reconstructed tracks;
- A wide window for the invariant mass cut so that the $\pi^+\pi^-$ mass spectrum may be reconstructed offline between 4.6 and 6.0 GeV for fitting purposes. This window corresponds to about $\pm 10\sigma(m_{Bd})$ which is 70 MeV offline.

Note that the second requirement means that other interesting channels such as $B_d \to \pi^+K^-$ will also be accepted. The full composition of the mass distribution obtained offline with a $\pi^+\pi^-$ hypothesis is shown in the Physics TDR [6].

6.3.1 Track selection

The track selection cuts used are as follows:

- .Si Kalman track $p_T > 3.9$ GeV.

- The trigger muon and Si Kalman track must be separated by at least $\Delta R=0.2$.

Table 11: This table shows the beneficial reduction in track candidates from each stage of the track selection. At each stage the efficiency (ε) to reconstruct both pions from the $B_d \to \pi^+\pi^-$ decay is also given. Note that without muon guidance, the pixel scan is actually less efficient. The number of tracks after the pixel track p_T cut (first row) is important for the Si Kalman algorithm time as it sets the number of pixel seeds to be followed by this algorithm.

	pixel-guided ΔZ_μ < 1 cm		**pixel-guided ΔZ_μ < 0.4 cm**		**TRT-LUT-guided**		**TRT-XK-guided**	
Track selection	**Mean no. tracks**	**ε (%)**	**Mean no. tracks**	**ε (%)**	**Mean no. tracks**	**ε (%)**	**Mean no. tracks**	**ε (%)**
Pixel track pT > 0.5 GeV	39.4	90.4%			132	78.9%	107.7	79.5%
Si Kalman track found from pixel seed	35.1	84.5%			56.7	72.6%	53.5	75.0%
Si Kalman track passes additional track selection (pT > 3.9 GeV, ΔR > 0.2)	2.1	*break-down below*			2.7	*break-down below*	2.5	*break-down below*
pT > 3.9 GeV		83.3%				68.3%		69.9%
ΔR > 0.2		80.9%				66.8%		68.1%

6.3.2 Selection

Tracks surviving the selection described in above are combined in all possible oppositely charged pairs. These pairs must then survive the selection cuts on the scalar sum of their transverse momenta, the difference between Z_0 of the two tracks, and a loose mass window cut. The mass window is chosen to be $\pm 10\sigma(mB_d)$ using the online resolution obtained with the pixel-guided Si-Kalman tracking, which is about 100 MeV. The effects of these cuts are shown in

Table 12. It should be noted that the background efficiencies suffer from very low statistics, as the errors indicate. For example, only 15 out of 1607 events survive the cuts on pixel-guided #1 tracks. [FIND A BETTER WAY OF PUTTING THIS!].

Table 12: Cuts to select track pairs that form good $B_d \to \pi^+\pi^-$ candidates. All numbers are efficiencies in (%).

	pixel-guided ΔZ_μ < 1 cm			**pixel-guided ΔZ_μ < 0.4 cm**		
Track pair selection	**Signal sample**	**Offline sample**	**$B \to \mu X$ sample**	**Signal sample**	**Offline sample**	**$B \to \mu X$ sample**
Track cuts (see Table 11)	90.1	97.3	18.8			
$p_T^+ + p_T^- > 10$ GeV	86.4	96.9	15.0			
$\|\Delta Z0\| < 2$ cm	86.4	96.9	15.0			
4.3 < mass < 6.3 GeV	77.7	93.5	$0.93^{+0.31}_{-0.24}$			
	TRT-LUT-guided			**TRT-XK-guided**		
Track pair selection	**Signal sample**	**Offline sample**	**$B \to \mu X$ sample**	**Signal sample**	**Offline sample**	**$B \to \mu X$ sample**
Track cuts (see Table 11)	82.3	86.4	24.8	82.6	88.8	24.0
$p_T^+ + p_T^- > 10$ GeV	79.4	85.7	21.3	79.1	88.4	20.3
$\|\Delta Z0\| < 2$ cm	74.9	81.8	14.7	76.0	85.5	15.5
4.3 < mass < 6.3 GeV	61.0	75.2	1.1±0.3	62.5	78.0	1.1±0.3

It may be noted that the track cuts give a higher efficiency for signal events than $B_d \to \pi^+\pi^-$ decays (contrast the top row of Table 12 with the bottom row of Table 11). This demonstrates that both signal and background events are at this stage selected because of combinatorial background as well as the correct reconstruction of the tracks from a $B_d \to \pi^+\pi^-$ decay. This is to be expected because the track selection alone is not specific to any particular B decay. The mass cut provides very specific selection of $B_d \to \pi^+\pi^-$ decays, as can be seen in Figure 13 (Pixel guided) and Figure 14 (TRT-XK guided). The plots for Pixel guided #2 and TRT-LUT guided respectively are similar.

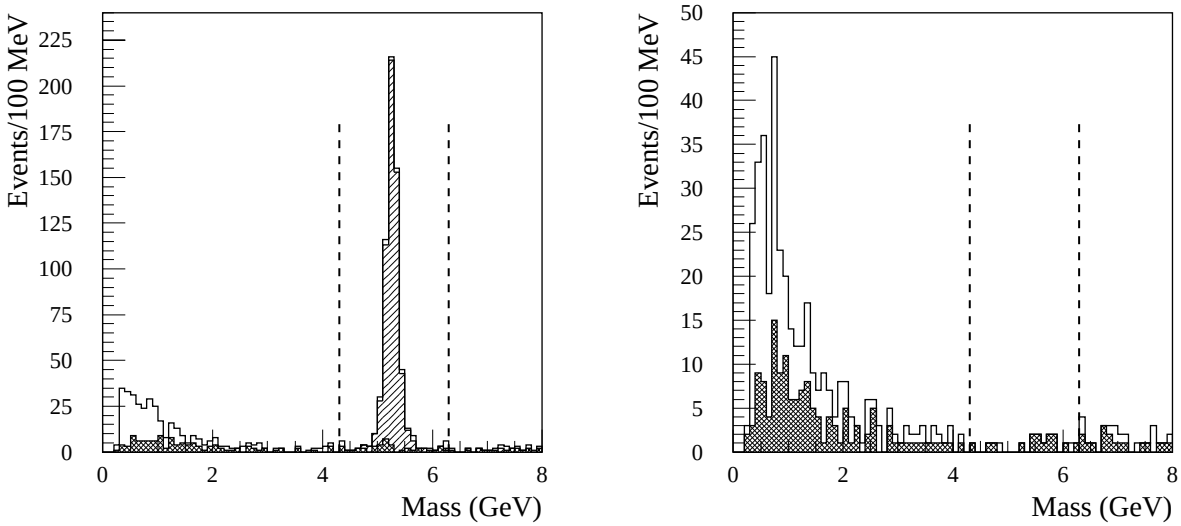

Figure 13: The distribution of invariant masses from oppositely charged track pairs from the pixel-guided tracking which survive the selection cuts in Table 12, in signal events (left) and background events (right). In both figures, the open histogram shows the mass distribution of all combinations of oppositely charged tracks, while the strongly-hatched histogram is limited to no more than one entry per event, and excludes (in the case of signal events) any combinations in which the tracks are associated to the two pions from the B_d decay. Only the pair nearest the centre of the B_d mass window is entered. For signal events there is also a lightly-hatched histogram on top of this which shows the mass when the pair of tracks are associated to the two pions from the B_d decay, also limited to no more than one entry per event. The mass cut window is shown by vertical dashed lines.

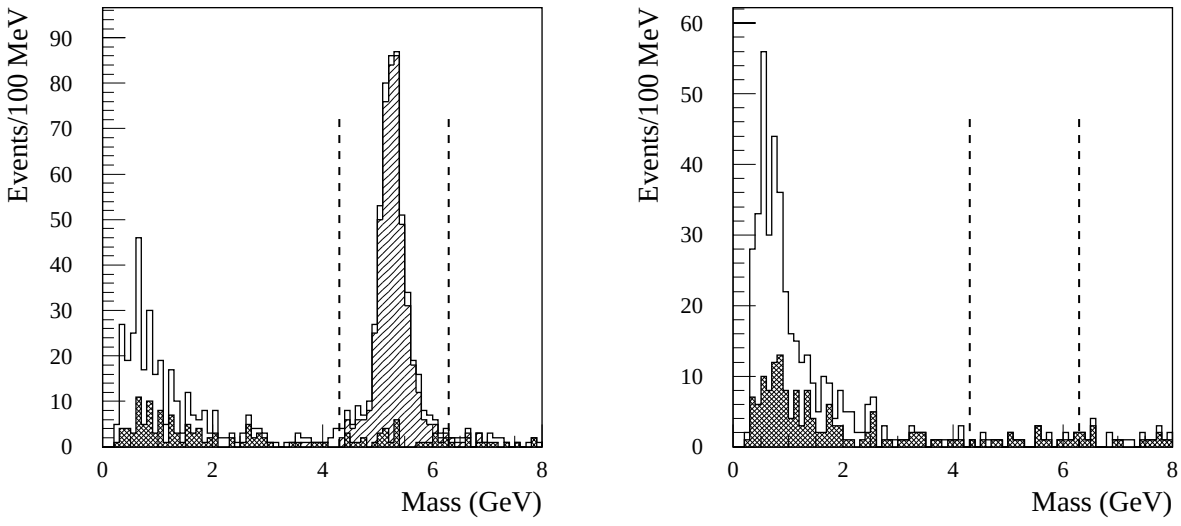

Figure 14: The distribution of invariant masses from oppositely charged track pairs from the TRTXK-guided tracking which survive the selection cuts in Table 12, in signal events (left) and background events (right). The key to the different histograms is the same as that explained in the caption of Figure 13.

The resulting signal efficiency and background rate are summarised in Table 13. The rate assumes an input rate to the LVL2 tracking trigger of 9 kHz. It is also assumed that this is dominated by $B \rightarrow \mu$X+pile-up or similar events. As explained in Section 4.1 this is probably pessimistic.

Table 13: Summary of $B_d \rightarrow \pi^+\pi^-$ trigger performance.

	pixel-guided ΔZ_μ < 1 cm	**pixel-guided ΔZ_μ < 0.4 cm**	**TRT-LUT guided**	**TRT-XK guided**
Efficiency to accept signal event	77.7%		61.0%	62.5%
Efficiency with respect to offline sample	93.5%		75.2%	78.0%
Rate from background events	84 Hz		100 Hz	100 Hz

The trigger efficiency has been checked as a function of the p_T and |η| of the B_d. This is shown in Figure 15, in which the pixel-guided Si-Kalman FEX was chosen as a representative example. The average efficiencies correspond to those in Table 13.

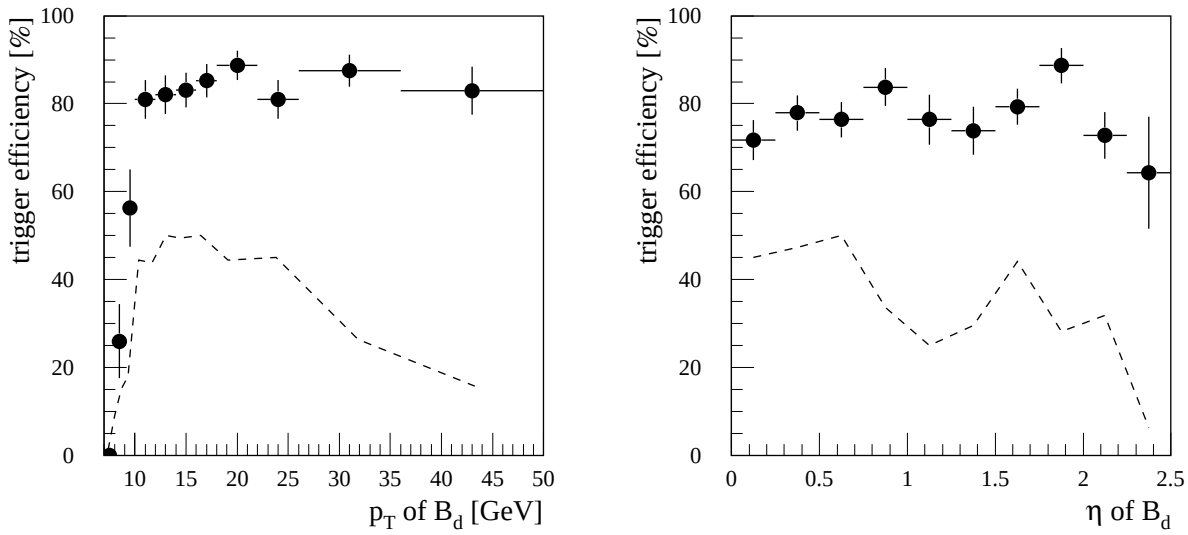

Figure 15: Efficiency to accept $B_d \rightarrow \pi^+\pi^-$ signal events as a function of the generated p_T (left) and |η| (right) of the B_d meson. Daughter pions are required to have p_T > 4.0 GeV. The dashed lines show the p_T (left) and |η| (right) distributions of the B_d meson. The general trend in the |η| distribution is fairly flat, falling off at high |η|; the detailed structure reflects the low statistics available. These plots were produced using the Pixel scan and Si-Kalman algorithms.

6.3.3 Event filter Selection

The EF selection differs from LVL2 in that the ID track reconstruction is performed using the offline program `xKalman` and a vertex fit is performed to pairs of tracks of opposite charge sign in order to reconstruct the decay vertex. The selection cuts are as follows:

- Invariant mass with-in the window 4.5 to 6.0 GeV
- Vertex fit has $\chi^2 < 8$
- reconstructed transverse decay length > 100 μm

- Cut on the angle in the transverse plane, α_T, between the vertex position vector and the direction of the reconstructed momentum vector, $\alpha<5^o$.

Using these cuts a gives a rate of 5 Hz (for a 9kHz μ6 rate). No events were rejected from the sample of events selected offline (note that the same reconstruction program was used for the offline analysis).

6.3.4 Conclusions

In this section, a viable $B_d \rightarrow \pi^+\pi^-$ trigger has been demonstrated. All algorithms gave a reasonable rate, but the pixel-guided tracking with $\Delta Z_\mu < 1$ cm gave the best efficiency. The rate and efficiency are comparable to those previously achieved using offline code (XKalman). The loss of events used by the offline analysis is minimal. The execution times of the algorithms used are reasonable and should be suitable for the LVL2 trigger, if processor speeds continue to increase as expected.

Selection cuts have been proposed for the event filter which can reduce the rate to about 5 Hz [18].

6.4 $D_s \rightarrow \phi^0(K^+K^-)\pi^-$

This channel is interesting for B_s mixing studies. The B_s decay is not completely reconstructed in the trigger, since the reconstruction of only the D_s decay is sufficient for rate reduction at LVL2. This allows more flexibility with inclusive selection of various $B_s \rightarrow D_s X$ decay channels, such as $B_s \rightarrow D_s\pi$, $B_s \rightarrow D_s a_1$, $B_s \rightarrow D_s D_s$ etc.

In principle, the decay mode $D_s \rightarrow K^{*0}(K\pi)K$ could also be reconstructed. A trigger for this mode would work similarly to the $D_s \rightarrow \phi^0(KK)\pi$ one, but preliminary studies [2] have shown that a reasonable trigger rate can only be obtained with a track-p_T cut of approximately $p_T > 3$ GeV. Moreover, due to the large width of the K^{*0}, the combinatorial background is dominant and hard to control.

The offline analysis requires that the trigger:

- has good efficiency for decays in which the three final-state daughters (K^+, K^-, π) have $p_T > 1.5$ GeV;
- reconstructs ϕ^0 candidates from two oppositely charged tracks (kaon mass hypothesis) in a relatively large mass window around the nominal ϕ^0 mass;
- reconstructs D_s candidates from two tracks which pass the ϕ^0 selection and a third track (pion mass hypothesis) in a relatively large mass ϕ^0 window around the nominal D_s mass.

The signal data set consists of 1989 fully simulated $B_s \rightarrow D_s\pi$ events with subsequent decay $D_s \rightarrow \phi^0(K^+K^-)\pi^-$, with the addition on pile-up at low-luminosity (the data sample was taken from the first 500 events of each of the files 37, 38, 53, 54 on tape Y24574 [16]). For the efficiency measurements, a sub-set of 821 events (denoted as KINE1.5) is obtained by requiring that there is exactly one B_s in the event and that the pions and kaons from the D_s decay have $p_T > 1.5$ GeV. As in the previous section, background refers to 1607 fully simulated $B \rightarrow \mu X$ events with low-luminosity pile-up added (from tape Y00347 [15]).

The offline analysis is used to define a smaller subset of the signal events.The offline-analysis cuts are those used in the $B_s \rightarrow D_s \pi / a_1$ analysis from the Physics TDR [4]. Details of these cuts are given in Appendix A.

6.4.1 Track selection

The track selection cuts applied are as follows:

- $d_0 < 1$ cm, $z_0 < 20$ cm
- $\Delta R > 0.2$.

Table 14 shows the reduction of the average number of tracks per event as a result of the above selection procedure and its effects on the efficiency for the signal data set. The number of tracks after the pixel-track p_T cut (in bold) is important for the execution time of the Si-Kalman algorithm, as it sets the number of pixel seeds to be followed by this algorithm.

Table 14: The number of track candidates and the efficiency to reconstruct all three final-state daughters from D_s with KINE $p_T > 1.5$ GeV, after each stage of the track selection.

	Pixel Guided				**TRT guided**			
	$\Delta z < 1$ cm $p_T > 0.5$ GeV		**$\Delta z < 0.4$ cm $p_T > 1.0$ GeV**		**TRT–LUT**		**TRT–XK**	
Track selection	**Mean no. tracks**	**ε (%)**	**Mean no. tracks**	**ε (%)**	**Mean no. tracks**	**ε (%)**	**Mean no. tracks**	**ε (%)**
Track $p_T > 0.5$ GeV	38.3	68.3	18.3	67.7	262	65.5	119	64.9
Si-Kalman track found from seed	34.6	56.5	17.4	60.2	86	57.0	64	59.8
Si-Kalman track passes track selection (no. space points ≥ 2, $p_T > 1.4$ GeV, $\Delta R > 0.2$)	7.8	55.3	7.1	58.7	16	54.6	12.5	57.5

Using the pixel seeded track search, on average, there are 7.1 remaining track candidates per event. The average efficiency to reconstruct tracks from D_s is 87.3% for pions and 77.2% for kaons, respectively (see Figure 16).

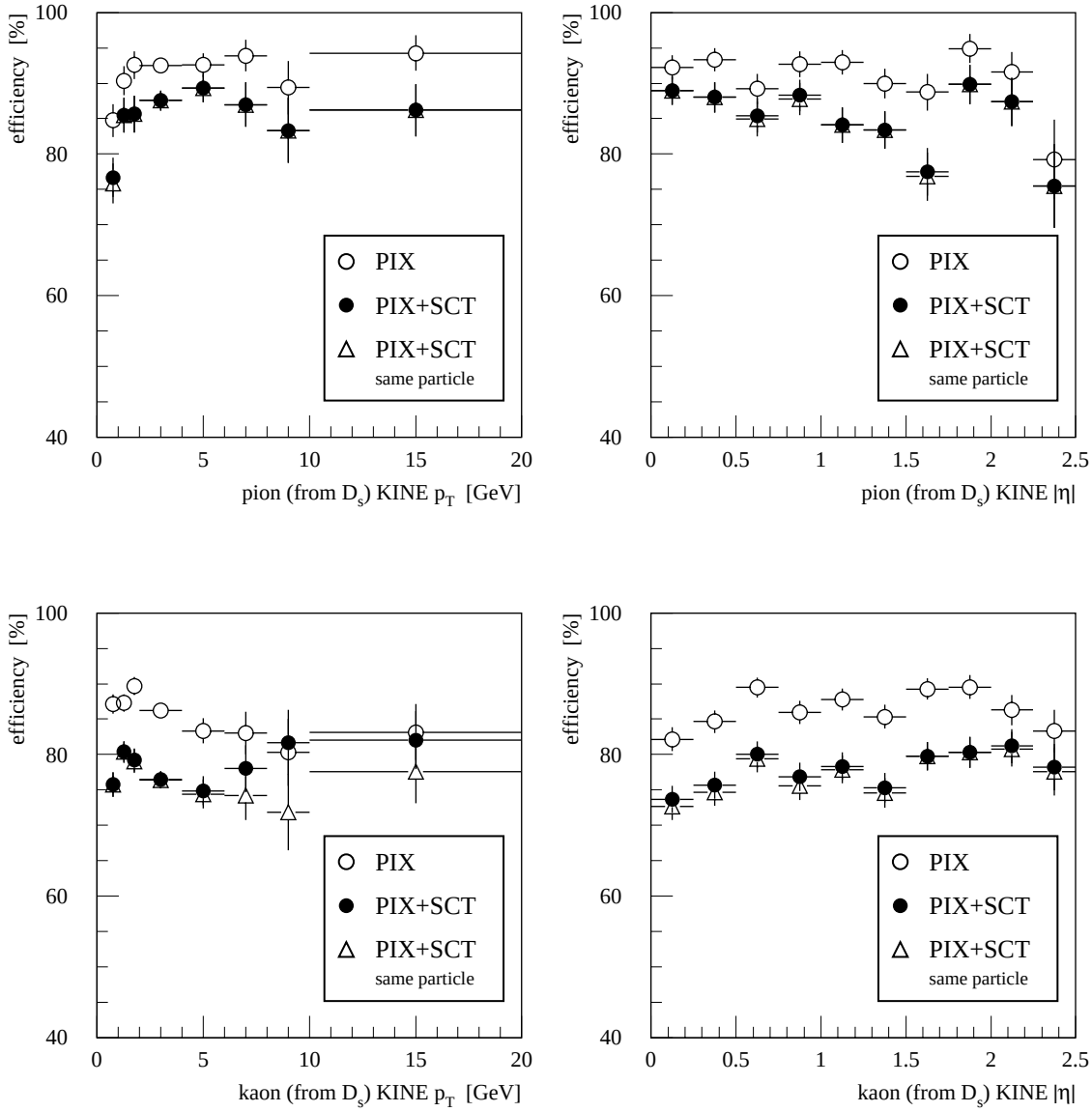

Figure 16: Track-reconstruction efficiencies for pions (top) and kaons (bottom) from the decay $D_s \rightarrow \phi^0(K^+K^-)\pi^-$ with $p_T > 0.5$ GeV versus KINE p_T (left) and KINE |η| (right) using the Si-kalman FEX seeded by a pixel-scan.

6.4.2 D_s reconstruction

From tracks satisfying the quality criteria of Section 6.4.1, oppositely charged track pairs are formed and their invariant mass is calculated, applying a kaon mass hypothesis for both tracks. Those track pairs whose invariant mass lies within a $5\sigma_{\phi}^{offl}$ mass window around the nominal ϕ^0 mass, i.e., $|M_{KK} - M_{\phi}| < 5\sigma_{\phi}^{offl}$, are selected as ϕ^0 candidates. Here, σ_{ϕ}^{offl} = 3.4 MeV is the ϕ^0 mass resolution obtained in offline analysis [6]. The resulting mass distribution in signal events is shown in Figure 17.

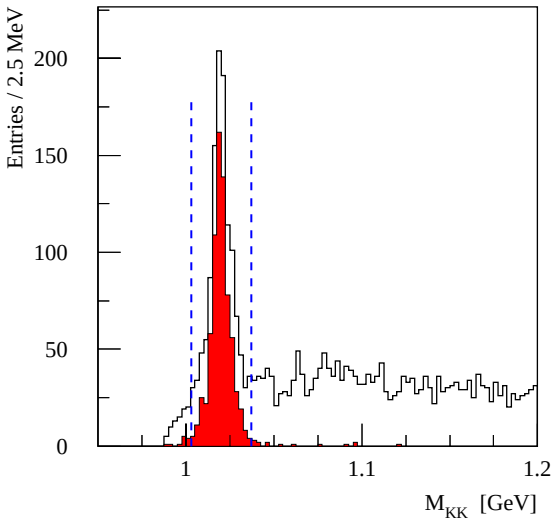

Figure 17: Reconstructed KK invariant-mass distribution. The $5\sigma_{\phi}^{offl}$ mass cut is indicated by the dashed lines. The dark histogram shows the candidates which match a generated ϕ^0.

These selected ϕ^0 candidates are then combined with all the remaining other tracks in turn, assuming the pion mass for the new track. Track triples whose combined invariant mass satisfies $|M_{KK\pi} - MD_s| < 5\sigma_{Ds}^{offl}$ are accepted as D_s candidates, where MD_s is the nominal D_s mass and σ_{Ds}^{offl} = 14.0 MeV is the D_s mass resolution obtained offline. The resulting mass distribution in signal and background events is shown in Figure 18.

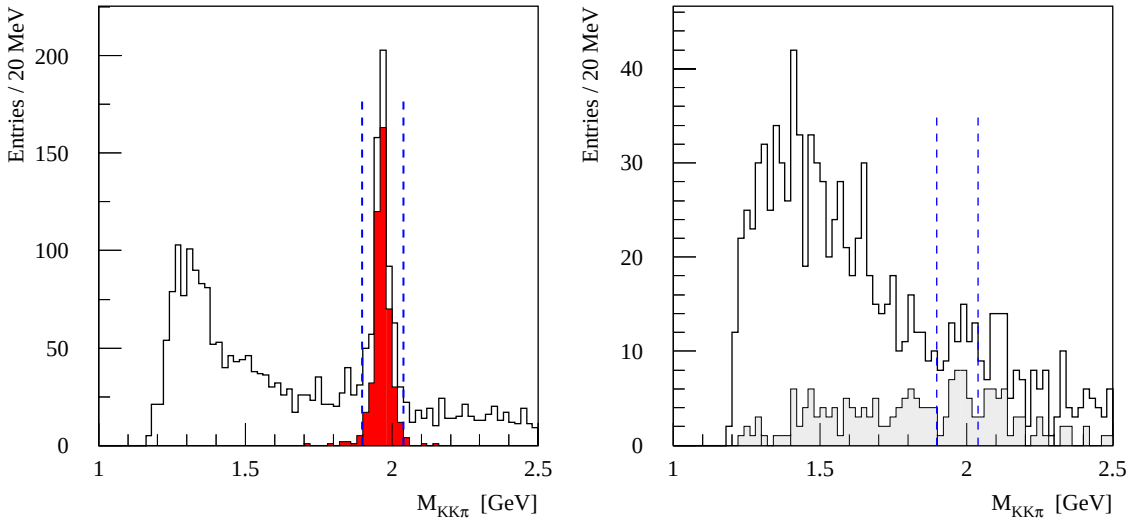

Figure 18: Reconstructed KKπ invariant-mass distribution. The $5\sigma_{Ds}^{offl}$ mass cut is indicated by the dashed lines. In the left plot, the dark histogram shows the candidates matching a generated D_s. In the right plot, the light-grey histogram shows the distribution when there is only (at most) one entry per event (i.e., the candidate closest to the nominal D_s mass).

Note that both for ϕ^0 and D_s selections, $5\sigma_{\phi}^{offl} \approx 3\sigma_{\phi}^{trig}$ and $5\sigma_{Ds}^{offl} \approx 3\sigma_{Ds}^{trig}$, where σ_{ϕ}^{trig} and σ_{Ds}^{trig} denote the trigger Si-Kalman mass resolutions for ϕ^0 and D_s. They have been determined by fitting with a single Gaussian the mass distributions of reconstructed candidates which match generated ϕ^0s and D_ss. In particular, σ_{ϕ}^{trig} = 5.1 MeV, σ_{Ds}^{trig} = 23.5 MeV.

The results of this selection procedure, both for signal and background events, are summarized in Table 15: The second line displays the events passing the muon trigger emulation described in Section 6.1. The third line (track cuts) refers to events containing at least three different reconstructed tracks (two oppositely charged, one of arbitrary charge) passing the track selection described in Section 6.4.1 .

Table 15: The effects of the cuts on the selection of D_S candidates for pixel-seeded searches.

		Pixel Guided		TRT Guided	
		$\Delta z < 1$ cm $p_T > 0.5$ GeV	$\Delta z < 0.4$ cm $p_T > 1.0$ GeV	TRT-LUT	TRT–XK
Efficiency (%)	π from Ds	87.7	84.6	81.5	83.0
	K from Ds	79.3	81.4	80.8	83.0
	ϕ	70.1	75.3	70.0	71.3
	Signal sample	58.2	62.6	54.1	54.3
	Offline sample	63.6	68.9	59.8	59.8
LVL2 Rate (Hz)		263	230	409	291

The efficiency for the ID to reconstruct the muon has been measured as 94.6% using the method described in Section 6.4.1; it is defined as the fraction of events in a given reference sample which pass the LVL2 muon trigger. Here, in order to use as high statistics as possible, all available 1989 events from the signal sample have been taken as reference sample.

The efficiency for signal events, (53.2%) is defined as follows: Those events out of the KINE1.5 sample which pass the LVL2 muon trigger (786 events) are taken as 100% reference sample. The fraction of events in this reference sample which pass the LVL2 D_s selection cuts (see above) is defined as KINE efficiency. (This definition is adopted to disentangle LVL2 trigger performance and muon-trigger emulation.)

The **LVL2 rate** (196 +39 / -33 Hz) is defined as the fraction of events out of the 1607 background events which pass both LVL2 muon trigger and D_s selection (see above), multiplied by the expected LVL2 input rate of 9000 Hz. The asymmetric errors are the binomial 68.3% confidence interval.

6.4.3 Effect of hit sharing.

As discussed in Section 6.3.1, whether or not track candidates are allowed to share hits is important in determining the mean number of tracks per event. It also has implications for the quality of the reconstructed tracks and hence the events selection efficiency and trigger rate. The effect of hit sharing is shown in Table 16 both for the case of an un-guided pixel search and a muon guided pixel search. In both cases the reconstruction efficiency is increased when hit sharing is allowed, but with a corresponding increase in trigger rate.

Table 16: The mean number of pixel seeds in $B \rightarrow \mu X$ events with pile-up for the cases when hit sharing is and is not allowed and the corresponding efficiency for reconstructing tracks in $D_s \rightarrow \phi^0(K^+K^-)\pi^-$ events with pile-up.

		No muon Guidance		With Muon Guidance (Δz<0.4cm)	
Efficiency		No hit sharing	With hit Sharing	No hit sharing	With hit Sharing
Mean No. Tracks		38	90	18	36
Efficiency (%)	π from D_s	85.2	86.7	84.6	85.2
	K from D_s	80.4	87.4	81.4	86.4
	φ	74.4	85.6	75.3	83.8
	Signal sample	60.1	73.1	62.4	72.0
	Offline sample	68.3	82.6	68.3	80.8
LVL2 Rate (Hz)		263	526	230	403

6.4.4 Comparison with offline

The offline selection is described in Appendix A. In offline analysis, one starts with the whole signal sample, which has been generated with a general cut of p_T(KINE) > 0.5 GeV for all the tracks from the *B* tree. During the analysis, no cuts on KINE level are imposed. The cut of p_T > 1.5 GeV for the three tracks used to find the D_s candidates is imposed on the reconstructed tracks, therefore one can have B_s or D_s candidates which pass all the selection cuts but have one or more tracks with p_T(KINE) < 1.5 GeV due to the resolution. This implies that for comparison between trigger and offline the whole signal sample is more appropriate to be taken as a reference sample than the KINE1.5 sample defined in Section 6.4.

In order to keep the rate for the LVL2 $D_s \rightarrow \phi^0(KK)\pi$ trigger as low as possible and without imposing too tight (ϕ^0, D_s) mass and p_T cuts, a separation cut between reconstructed tracks and the reconstructed trigger-muon track (ΔR > 0.2, cf. Section 6.4.1) had to be introduced. This separation cut, as well as the muon trigger emulation, has no counterpart in offline analysis. In order to find an appropriate trigger / offline efficiency, it is therefore necessary to disentangle the effects due to trigger performance and those introduced by the crude muon-trigger emulation. For this purpose, those events which pass the offline selection but not the crude muon trigger are rejected.

From the 1989 events of the signal sample, there are 175 events which pass the full offline selection; 166 out of them pass the crude LVL2 muon trigger. 495 events out of the signal sample pass the LVL2 trigger selection (muon trigger included), 92 of them are common LVL2 / offline events. The **offline efficiency** is therefore 92 / 166 = 55.8%.

Due to the incomplete reconstruction of the $B_s \rightarrow D_s\pi$ decay in the LVL2 trigger, one could also calculate an offline efficiency with respect to D_s, taking events which pass the offline cuts up to and including the $3\sigma_{Ds}$ mass cut as a reference sample. There is no counterpart in the $B_d \rightarrow \pi\pi$ channel, where the whole decay is reconstructed in LVL2. This D_s offline efficiency is closer to the trigger selection, since the B_s selection is not taken into account, but it is of little use for the offline analysis. From the 821 events of the KINE1.5 sample, there are 536 events which pass the D_s offline selection; 515 out of them pass the crude LVL2 muon trigger. 294 events are common LVL2 / offline events. The D_s **offline efficiency** is therefore 294 / 515 = 57.1%.

The rather low offline efficiency (compared to the $B_d \rightarrow \pi\pi$ channel, Section 5.4), seems to be due to the different track-reconstruction algorithms in LVL2 (pixel-guided Si-Kalman filter) and offline (xKalman), manifest at least for lower-p_T tracks. More investigations on this issue are needed.

In offline studies, the appropriate correction factor to be applied for the LVL2 trigger efficiency is then: muon efficiency (cf. Section 6.3) times offline efficiency, i.e., 52.7%.

6.4.5 Event Filter Selection

The ID track reconstruction is performed using the offline program `xKalman and a` vertex fit is performed firstly to pairs of tracks of opposite charge sign in order to reconstruct the ϕ decay vertex and then a third track is added to the fit to reconstruct the D_s decay vertex. The selection cuts are as follows:

- Invariant mass of track pair with-in the window 999 to 999 GeV
- two-track vertex fit has $\chi^2 < 6$
- Invariant mass of track-triplet in window 999 to 999 GeV
- reconstructed transverse decay length of $D_s > 180\ \mu m$
- Cut on the angle in the transverse plane, α_T, between the D_s vertex position vector and the direction of the reconstructed D_s momentum vector, $\alpha<20^o$.

Using these cuts a gives a rate of 50 Hz (for a 9kHz μ6 rate). No events were rejected from the sample of events selected offline (note that the same reconstruction program was used for the offline analysis).

6.4.6 Conclusions

In this section, a viable $D_s \rightarrow \phi^0(K^+K^-)\pi^-$ trigger, both in rate and efficiency, has been demonstrated.

6.5 $J/\psi \rightarrow e^+e^-$

The channel $B_d \rightarrow J/\psi(e^+e^-)K_S$ is important as it provides a clean measurement of the angle β of the unitarity triangle. It is important that the trigger:

- provides good efficiency for electron tracks down to ~1 GeV (this implies a p_T threshold of 0.5 GeV)
- makes use of the electron identification capability of the TRT in order to reduce the combinatorial background from hadron tracks.

These requirements pose a challenge for the trigger for the following reasons:

- The effect of Bremsstrahlung energy loss means that reconstruction of electron tracks is more difficult a task than reconstruction of muons or hadrons.

- The lower p_T threshold means that the effects of multiple scattering are more significant than for the other channels discussed in this note.
- If a pixel seeded search is used, an extra step is required to associate TRT information with the Si track. This step can potentially result in miss-association or loss of efficiency.
- If a TRT seed is used, energy loss before the TRT can cause kinks in the track which adversely affect the prolongation of the track into the Si detector.

Two approaches, using both a pixel-guided and TRT-guided search have been followed for this channel. In addition performance has been measured for both the TRT-LUT and TRT-XK algorithms.

6.5.1 Electron track finding and identification

The electron reconstruction performance of the various algorithms was discussed in Section 5. A summary is given in Table 17. of the mean number of tracks in $B \rightarrow \mu X$ events with pile-up

Table 17: Track selection results for a TRT-seeded search. The mean number of tracks passing the sequential selection steps in $B \rightarrow \mu X$ events and the corresponding efficiency to reconstruct both e^+ and e^- from $J/\psi \rightarrow e^+e^-$ events with electron $p_T^{true} > 1$ GeV. Pile-up at low luminosity was applied to both event samples. Results are shown for the TRT-XK and TRT-LUT FEX.

	TRT-XK		**TRT-LUT**	
Track selection	**Mean no. of tracks**	**Efficiency (%)**	**Mean no. of tracks**	**Efficiency (%)**
TRT scan, p_T>0.5 GeV	120	83	171	
TRT tracks identified as e	24	65	57	
Si Kalman tracks from e seed	7.2	57		
Si Kalman track with *B*-layer hit	5.8	52		

passing each successive selection step and the corresponding efficiency to reconstruct both electrons from $B_d \rightarrow J/\psi(e^+e^-)K_S$ events with pile-up. electron $p_T^{true} > 1$ GeV. Results are shown for the TRT-XK and TRT-LUT FEX. The track cuts are as follows:

- TRT track reconstructed with $p_T > 0.5$ GeV
- TRT track passes electron identification cuts, see Table 4. A cut is applied to the ratio $R=N_{TR}/N_{hits}$ where N_{hits} is the total number of TRT hit son the track and N_{TR} is the number of hits passing a higher read-out threshold indicating transition radiation.
- Si-Kalman track reconstructed from TRT seed

- Si track contains a *B*-layer hit

Table 18: Track selection results for pixel-seeded search. The mean number of tracks passing the sequential selection steps in $B \rightarrow \mu X$ events and the corresponding efficiency to reconstruct both electrons from $J/\psi \rightarrow e^+e^-$ events with electron $p_T^{true} > 1$ GeV. Pile-up at low luminosity was applied to both event samples. Results are shown for the TRT-LUT FEX.

Track selection	**Mean no. of tracks**	**Efficiency (%)**
pixel scan, p_T>0.5 GeV	114	
Si Kalman tracks from e seed		
Si Kalman track with *B*-layer hit		
Associated TRT track		
Associated TRT track identified as electron		

. The mean number of tracks is lower for the TRT-XK FEX for two reasons:

- the TRT-LUT FEX has been tuned to preserve efficiency in the barrel to end-cap transition region, and
- the TRT-XK FEX incorporates a step to resolve sharing of hits between different tracks

6.5.2 Track pair selection

Table 19: The R_{12} cut value used for e^+e^- pair identification as a function of $|\eta|$ of the e- and e+. The track pair is considered as an e^+e^- pair if the value of R12 is greater than the cut given in the table.

	$\|\eta\| <$ **0.8**	**0.8** $< \|\eta\| <$ **1.4**	**1.4** $< \|\eta\| <$ **2.0**	**2.0** $< \|\eta\|$
$\|\eta\|$ **< 0.8**	0.15	0.18	0.20	0.20
0.8 < $\|\eta\|$ **< 1.4**	0.18	0.18	0.20	0.20
1.4 < $\|\eta\|$ **< 2.0**	0.20	0.20	0.20	0.22
2.0 < $\|\eta\|$ **<**	0.20	0.20	0.22	0.22

The tracks surviving the above cuts are combined in all charged-pair combination and the following cuts are applied:

- electron pair identification cut R_{12}, see Table 19;
- Difference in pseudo-rapidity between two tracks, $|\Delta\eta| < 1.5$
- Sum of transverse momenta, $p_T^+ + p_T^- > 3$ GeV
- Difference in Z intercept of two tracks, $\Delta Z_0 < 2$ cm

- The effective mass of the track pair, using an electron hypothesis is in window 2 GeV < M < 3.8 GeV

Table 20: Event selection results for TRT-seeded search. The effect of the sequential selection cuts for $B_d \rightarrow J/\psi(e^+e^-)K_S$ events with electrons with $p_T^{true} > 1$ GeV (signal sample), $B_d \rightarrow J/\psi(e^+e^-)K_S$ events selected offline (offline sample), and background, $B \rightarrow \mu X$ events.

	TRT-XK			TRT-LUT		
	Signal sample	**offline sample**	**$B \rightarrow \mu X$ events**	**signal sample**	**offline sample**	**$B \rightarrow \mu X$ events**
Track cuts (see Table 17)	85	87	69	96		93
electron pair id: $R_{12} > R_{cut}$	81	84	54	91		80
$\|\Delta\eta\| < 1.5$	77	81	47	90		76
$p_T^+ + p_T^- > 3$GeV	70	77	28	82		50
$\|\Delta Z_0\| < 2$ cm	64	71	22	75		41
2 < mass < 3.8 GeV	51	62	11	56		22
$\|\Delta\eta\| < 1.4$	76	80	46			
$p_T^+ + p_T^- > 4$ GeV	64	74	22			
$\|\Delta Z_0\| < 2$ cm	58	67	17			
2 < mass < 3.5 GeV	44	57	5.2			
cos(φ) > 0.2	43	56	4.1			

Table 21: Event selection results for a pixel-seeded search. The effect of the sequential selection cuts for $B_d \rightarrow J/\psi(e^+e^-)K_S$ events with electrons with $p_T^{true} > 1$ GeV (signal sample), $B_d \rightarrow J/\psi(e^+e^-)K_S$ events selected offline (offline sample), and background, $B \rightarrow \mu X$ events.

	signal sample	**offline sample**	**$B \rightarrow \mu X$ events**
Track cuts (see Table 18)	95		91
electron pair id: $R_{12} > R_{cut}$	89		77
$\|\Delta\eta\| < 1.5$	87		74
$p_T^+ + p_T^- > 3$GeV	76		42
$\|\Delta Z_0\| < 2$ cm	72		37
2 < mass < 3.8 GeV	58		24

6.5.3 Event filter Selection

ID track reconstruction is performed using the offline program `xKalman and a` vertex fit is performed to e^+e^- pair candidates in order to reconstruct the decay vertex. The selection cuts are as follows:

- Invariant mass with-in the window 2.5 to 3.4 GeV

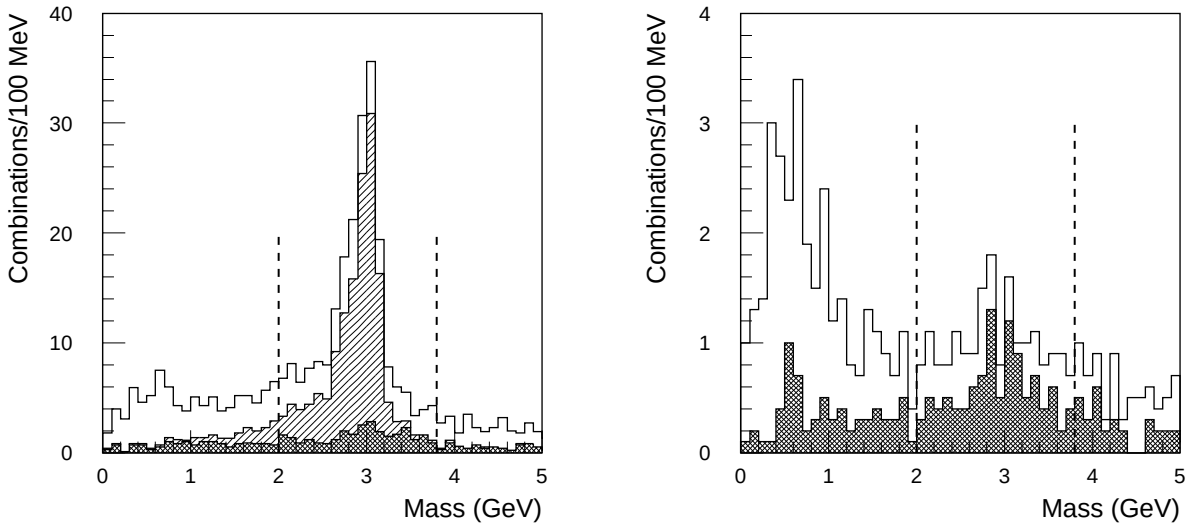

Figure 19: The invariant mass peak for opposite charge sign pair combination in the signal (left) and background (right). Results are shown for the Si-kalman FEX seeded by the TRT-XK FEX top and by the TRT-LUT FEX bottom.

- Vertex fit has $\chi^2 < 8$
- reconstructed transverse decay length > 180 μm
- Cut on the angle in the transverse plane, α_T, between the vertex position vector and the direction of the reconstructed momentum vector, $\alpha<40^o$.

Using these cuts a gives a rate of 30 Hz (for a 9kHz μ6 rate). No events were rejected from the sample of events selected offline (note that the same reconstruction program was used for the offline analysis).

6.6 Summary of HLT selections

Table 22: Performance summary for the *B*-physics HLT. The efficiencies for the signal samples and the efficiencies for signal events selected offline are given for each channel after LVL2 and after the LVL2 and EF selections. Also given are the rates and execution times for *B*->μX events with pile-up. The results have been obtained with the Si-FEX seeded by a pixel-scan for $B_d \rightarrow \pi^+\pi^-$ and $D_s \rightarrow \phi(K^+K^-)\pi$ and seeded by the TRT-XK FEX for $J/\psi \rightarrow e^+e^-$. The rates quoted are for a 9 kHz LVL2 muon rate. LVL2 execution times were measured on a 600 MHz AMD Athlon. The EF execution time is based on the execution time for the offline reconstruction program xkalman.

	LVL2				LVL2 + EF		
Trigger	ε^{α} **(%)**	**ε w.r.t. offline (%)**	**Rate (Hz)**	**Time (ms)**	**ε w.r.t. offline (%)**	**Rate (Hz)**	**Time (s)**
$B_d \rightarrow \pi+\pi-$	78	94	78	40	94	5	~10
$D_s \rightarrow \phi(K^+K^-)\pi$	56	56	196	40	56	27	~10
$J/\psi \rightarrow e^+e^-$	46	62	860	430	62	56	~10

a. Efficiencies for: $B_d \rightarrow \pi^+\pi^-$ events with pion $p_T > 4$ GeV, $D_s \rightarrow \phi(K^+K^-)\pi$ events with all three final state tracks with $p_T > 1.5$ GeV and $J/\psi \rightarrow e^+e^-$ events with electron $p_T > 1$ GeV.

6.7 Robustness

It is important that the trigger is robust with respect to detector inefficiency, noise and miss-alignment. The data-sets used in this study contain a simulation of detector inefficiency (3% for the SCT, TRT and Pixels) and of the expected levels of front end electronic noise in the SCT and Pixels. The effects of detector miss-alignment were not simulated at the generation stage, but have been simulated by displacing the reconstructed points which form the input to the FEX algorithms. In a preliminary study, miss-alignment of the SCT and Pixel detectors using Gaussian distributions equal in width to the intrinsic detector resolutions causes no change in efficiency or rate. Increasing the level of miss-alignment by a factor of three causes a loss of efficiency for the $B_d \rightarrow \pi^+\pi^-$ trigger of ~10% without change in the trigger rate.

7 Summary and conclusions.

Table 23: Summary of trigger rates and efficiencies obtained using the selections described in this note.

Trigger requirements		Selected B-channels	Rate (Hz)	
			LVL2	Event Filter
Hadron channels	$D_s \rightarrow \phi(K^+K^-)\pi$, 3 hadrons $p_T > 1.5$ GeV, loose mass cuts	$B_s \rightarrow D_s\,\pi$, $B_s \rightarrow D_s\,a_1$	230	27
	2 hadrons $p_T > 4$ GeV, loose mass, angle and $\sum p_T$ cuts	$B_d \rightarrow \pi\pi$ $B_d \rightarrow K\pi$	80	5
Electron channels	ee pair, $p_T > 0.5$ GeV, identification by TRT, 2.0 GeV < m(ee) < 3.8 GeV	$b\bar{b} \rightarrow \mu B_d(J/\psi(ee)K^0)$	860 (369)	56
Other channels not covered in this note			263	
Total LVL2 B-physics trigger rate			1170 (942)	

Previous measurements of the performance of a B-physics trigger were based on offline code [3]. Comparable performance has now been obtained for the $B_d \rightarrow \pi^+\pi^-$ and $B \rightarrow D_s(\phi(KK)\pi)\pi$ selections using algorithms suitable for the LVL2 trigger. Good progress has also been made with algorithms for the $B \rightarrow J/\psi(e^+e^-)$ channel, however these studies are at a relatively early stage. For this channel, a LVL2 rate 2.8 times higher than that reported in Ref. [3] is obtained using the same selection cuts (for 6% higher efficiency). It is possible to obtain performance approaching that reported in Ref. [3] using different selection cuts, the rate is given in brackets in Table 23. A possible event filter selection has been proposed giving a factor ~10 reduction in trigger rate without loss of signal events which would be selected offline. A preliminary study has shown the B-physics trigger to be robust with respect to the expected levels of miss-alignment in the SCT and Pixel detectors.

8 References

1 A. Di Mattia, A. Nisati, S. Robins, *Combined muon reconstruction at Level-2*. ATLAS Internal Note ATL-COM-DAQ-2000-024 (Mar 2000)

2 The ATLAS collaboration, *ATLAS Inner Detector Technical Design Report Volume I*, ATLAS TDR 4, CERN / LHCC 97-16 (April, 1997)

3 The ATLAS collaboration, *ATLAS Trigger Performance Status Report*, CERN / LHCC 98-15 (June, 1998).

4 Smizanska, M; Baranov, S.P.; Hrivnac, J.; Kneringer, E. *Overview of simulations for ATLAS B-physics studies* ATL-COM-PHYS-99-042

5 Flora Rizatdinova, Semi-inclusive *B*-physics triggers at low luminosity, ATL-DAQ-98-114 (1998).

6 The ATLAS Collaboration, ATLAS detector and physics performance TDR, CERN-LHCC-99-15 (1999).

7 P. Billoir, Nucl. Inst. and Meth. 225 (1984) 352., P. Billoir and S. Qian, Nucl. Inst. and Meth. A294 (1990) 219 and A295 (1990) 492.

8 J. Baines et al., Pattern Recognition in the TRT for the ATLAS *B*-Physics Trigger, ATL-DAQ-99-007 (1999).

9 I. Gavrilenko, Description of Global Pattern Recognition Program (XKalman), ATL-INDET-97-165 (1997).

10 S. Gonzalez and S. Qian, Si Kalman FEX note, ATL-DAQ-? (2000).

11 .A. Baratella, M. Dameri, P. Morettini and F. Parodi, *PixTrig: a track finding algorithm for LVL2*, ATLAS-COM-DAQ-2000-010 (2000).

12 L. Guy, PhD Thesis or ATLAS note in preparation (2000).

13 W. Li and S. George, ATLAS note in preparation (2000).

14 R. Dankers and J. Baines. A Data Preparation Algorithm for the Precision Tracker LVL2 FEX, ATL-DAQ-99-001 (1999).

15 *B*-physics tapes with minimum bias, `http://home.cern.ch/~msmizans/production/tapelist_minb.html`.

16 Innsbruck Monte Carlo production: *B*-physics simulation http: / / home.cern.ch / ~emo / b_sim.html

17 D. Rousseau, private communication.

18 F. Rizatdinova, N. Nikitin, *Rejection of rate at EF for J/Ψ, Ds and* $B_d \rightarrow \pi^+\pi^-$ *channels* ATLAS Internal Note, ATL-COM-DAQ-2000-017 (2000).

19 Y. Coadou, J. Damet, H. Korsmo, G.F. Tartarelli, *Measurement of sin(2beta) from* B^0_d*->J/Ψ* K^0_s ATLAS Internal Note ATL-PHYS-99-022 (1999).

Appendix A: Offline Selections

$B_d \rightarrow \pi^+\pi^-$

The offline event selection [17] is as follows:

- for the event
  - only two *B* mesons generated in the event
  - one $B_d \rightarrow \pi^+\pi^-$ decay
  - a muon trigger, which is simulated by requiring a muon generated within $|\eta| < 2.4$, p_T>6 GeV, successfully reconstructed in ID with a *B*-layer hit. Note no muon system simulation / reconstruction was used explicitly.
  - the two pions come directly from the *B*, not from hadronic interactions.
- for both pion candidates
  - Pt>4 GeV
  - impact parameter greater than 3 sigma
  - at least 9 Si hits including a *B*-layer hit
  - $\Delta R(\pi,\mu) > 0.4$ or Mass(π,μ) > 5 GeV
  - exclude candidate if a third track (X) is found which satisfies:
    - delta R (X,π)<1
    - M (X,π)<5.5 GeV
    - p_T > 1 GeV
    - no. of Si hits > 8
  - and one of the following two sets of condition
    - - vertex consistency: Mass(X, π^+, π^-) < 5.5 GeV and impact parameter of X w.r.t. $\pi^+\pi^-$ vertex less than 3 σ
    - - track consistency: mass(X,pion)<2; delta R (X,pion)<0.5; vertex probability>1%; decay-length greater than 10 sigma

  (These complicated cuts are needed to reject bad combinations and *B*->h^+h^-X decays. They have been optimized but there may still be scope for further improvement.)
- for the $\pi\pi$ combination
  - opposite charge
  - sum Pt >10 GeV
  - $\pi\pi$ 3D vertex probability >5%
  - decay length greater than 3 sigma
  - $\pi\pi$ 2D momentum consistency with beam-line and secondary vertex fit probability > 5%

- No mass cuts (except 4.5 - 6 GeV window) are applied because the mass histogram is fitted.

$D_s \rightarrow \phi^0(K^+K^-)\pi^-$

Unlike the analysis in [6], the offline analysis is restricted to events which contain only one $B_s \rightarrow D_s(\phi^0(KK)\pi)\,\pi$ decay. Events with two or more B_s mesons (not necessarily decaying into the $D_s(\phi^0(KK)\pi)\,\pi$ channel) are excluded.

The ϕ^0 is reconstructed from two oppositely charged tracks taken from the sample of tracks reconstructed by xKalman. A kaon mass hypothesis is applied for each track, and track pairs are selected which meet the following additional requirements:

- $p_T > 1.5$ GeV for each track
- angular cuts: $\Delta\phi_{KK} > 10^0$, $\Delta\theta_{KK} > 10^0$
- vertex-fit probability greater that 1%
- invariant mass within $3\sigma_\phi$ of the nominal ϕ^0 mass

The accepted ϕ^0 candidates are combined with a third track (pion mass hypothesis) with $p_T > 1.5$ GeV, and a three-track vertex is refitted. The combinations passing a vertex-fit probability cut of 1% and having an invariant mass within a $3\sigma_{Ds}$ mass window around the nominal D_s mass are selected as D_s candidates.

In offline analysis, the D_s candidates are combined with a fourth track with $p_T > 1.5$ GeV, assumed to be a pion. The four-track combination is subjected to the following selection procedure/cuts:

- The B_s vertex is refitted using ϕ^0 and D_s mass constraints, requiring a vertex-fit probability greater than 1%. The reconstructed B_s vertex should points back towards the primary vertex and the D_s vertex back to the B_s vertex.
- B_s proper time > 0.4 ps
- B_s impact parameter < 55 μm
- B_s $p_T > 10$ GeV
- invariant mass within $2\sigma_{Bs}$ of the nominal B_s mass

The last cuts in the B_s selection above have no correspondent in the LVL2 trigger selection procedure, which reconstructs D_s candidates only.